

**INVESTIGATING THE OPTICAL BAND GAP AND  
CRYSTAL STRUCTURE OF COPPER SULPHIDE AND  
COPPER SELENIDE THIN FILMS DEPOSITED BY  
CHEMICAL BATH DEPOSITION**

KNUST

By

Danu Bernice Yram, BSc. Physics

A Thesis submitted to the Department of Physics, Kwame Nkrumah University of  
Science and Technology, in partial fulfillment of the requirement for the degree of

MASTER OF PHILOSOPHY (SOLID STATE PHYSICS)

Department of Physics,

College of Science

APRIL, 2015



## ACKNOWLEDGEMENT

My first and foremost Thanks and Gratitude goes to the ALMIGHTY and EVER MERCIFUL GOD who in His infinite mercy and grace has brought me this far and given me the strength, knowledge and self- confidence to complete this work.

I continue to express my sincere appreciation to my thoughtful and motivating supervisor, Dr. Francis Kofi Ampong and Co-supervisor, Mr. Isaac Nkrumah for their guidance and effective supervision throughout this thesis. I am immensely grateful to them.

Furthermore, I express my sincere thanks to the Department of Physics, University of Ghana especially, Dr. Martin Egblewogbe (lecturer in-charge of the XRD laboratory), Dr. Amos Kuditcher (Head of Physics Department), and Elena (Laboratory technician) for their help in acquiring some of the data needed for this work.

I will also like to thank Professor Francis Boakye, Professor R. Nkum, Charles Bandoh, Fekadu Geshaw, Tizazu Abza, Emmanuel, Dr. Amekudzi, Mr. Amoah and Stephen Boandoh for their help one way or the other towards this thesis.

My heartfelt gratitude goes to my parents and siblings for their unending prayers and never failing support in all forms

## ABSTRACT

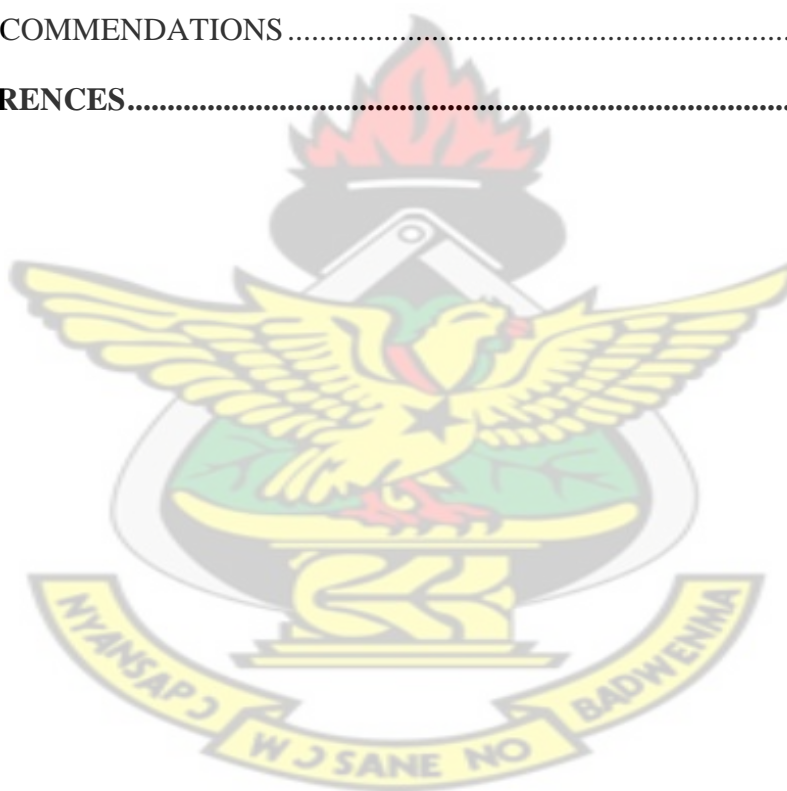
Thin films of CuS and CuSe have been successfully deposited using the CBD technique. The reagents used for the deposition of CuS were copper chloride, thiourea and ammonia. CuSe was deposited from chemical baths containing copper chloride, sodium selenosulphate and ammonia. The pH deposition temperature and time were optimized for deposition. The optical band gap and the structure of the as-deposited and annealed films were studied using optical absorption spectroscopy and powder x-ray diffraction analysis. The crystal structure of the as-deposited CuS films showed the presence of several phases with covellite being the dominant phase. After annealing at 673 K, only the copper sulphate pentahydrate phase was observed. The band gap varied from 1.6 eV for the as-deposited sample to 2.2 eV after annealing at 673 K. Optical studies on CuSe showed that the as-deposited films had two band gaps of 1.2 and 1.4 eV suggesting the presence of more than one phase. This feature was also observed in the samples annealed at 473 K, but samples annealed at 573 K and 673 K had only one band gap of 2.2 eV. The crystal structure of the as-deposited CuSe films showed the presence of several phases with the umangite being the dominant phase. However, after annealing at 673 K, the dominant phase was krutaite, suggesting a possible phase transformation.

## TABLE OF CONTENTS

|   |             |
|---|-------------|
| <b>DECLARATION.....</b>   | <b>ii</b>   |
| <b>ACKNOWLEDGEMENT.....</b>   | <b>iii</b>  |
| <b>ABSTRACT.....</b>  | <b>iv</b>   |
| <b>TABLE OF CONTENTS .....</b>  | <b>v</b>    |
| <b>LIST OF TABLES .....</b>   | <b>viii</b> |
| <b>LIST OF FIGURES .....</b>  | <b>ix</b>   |
| <b>LIST OF SYMBOLS AND ACRONYMS .....</b>   | <b>xi</b>   |
| <b>CHAPTER ONE .....</b>  | <b>1</b>    |
| <b>INTRODUCTION.....</b>  | <b>1</b>    |
| 1.1 COPPER SULPHIDE .....   | 3           |
| 1.2. COPPER SELENIDE.....   | 5           |
| 1.3 OBJECTIVE OF THE PROJECT .....  | 6           |
| 1.3.1. SPECIFIC OBJECTIVES .....  | 7           |
| 1.4. REASONS FOR INVESTIGATING THE OPTICAL PROPERTIES, CRYSTAL<br>STRUCTURE OF THE THIN FILM AND THE EFFECT OF ANNEALING..... | 7           |
| 1.4.1. JUSTIFICATION OF THE PROJECT.....  | 8           |
| 1.5. STRUCTURE OF THE THESIS .....  | 9           |
| <b>CHAPTER TWO .....</b>  | <b>10</b>   |
| 2.0 LITERATURE REVIEW .....   | 10          |
| 2.1. THIN FILM TECHNOLOGY .....   | 10          |
| 2.1.1. TYPES OF THIN FILM DEPOSITION TECHNIQUES .....   | 10          |
| 2.1.1.1. Chemical vapour deposition (CVD) .....   | 11          |
| 2.1.1.2. SILAR method (Successive Ionic Layer Adsorption and Reaction) .....  | 11          |
| 2.1.1.3. Chemical bath deposition (CBD).....  | 12          |
| 2.1.1.4. Electrophoretic deposition: .....  | 13          |
| 2.1.1.5. Sputtering:.....   | 14          |

|   |           |
|---|-----------|
| 2.2. REVIEW OF COPPER SULPHIDE THIN FILMS DEPOSITED BY CHEMICAL BATH TECHNIQUE..... | 15        |
| 2.3. REVIEW OF COPPER SELENIDE THIN FILMS DEPOSITED BY CHEMICAL BATH TECHNIQUE..... | 17        |
| <b>CHAPTER THREE.....</b>   | <b>20</b> |
| 3.0. THEORETICAL BACKGROUND.....  | 20        |
| 3.1. SEMICONDUCTORS.....  | 20        |
| 3.1.1. BASIC SEMICONDUCTOR CONCEPT.....   | 20        |
| 3.1.2. CLASSIFICATION OF SEMICONDUCTORS.....  | 22        |
| 3.2. BASIC PRINCIPLES OF CHEMICAL BATH DEPOSITION (CBD).....                        | 25        |
| 3.2.1. Nature of reactants/precursor concentration.....                             | 26        |
| 3.2.2. pH:.....   | 26        |
| 3.2.3. Deposition time.....   | 26        |
| 3.2.4. Nature of substrates.....  | 27        |
| 3.2.5. Complexing agent.....  | 27        |
| 3.3. BASIC MECHANISM OF CBD.....  | 27        |
| 3.4. THEORY OF THE CHARACTERIZATION TECHNIQUES.....                                 | 29        |
| 3.4.1. OPTICAL ABSORPTION.....  | 30        |
| 3.4.2. X-RAY DIFFRACTION.....   | 36        |
| <b>CHAPTER FOUR.....</b>  | <b>41</b> |
| 4.0. METHODOLOGY.....   | 41        |
| 4.1 SUBSTRATE PREPARATION.....  | 41        |
| 4.2 PREPARATION OF COPPER SELENIDE THIN FILMS.....                                  | 41        |
| 4.3 PREPARATION OF COPPER SULPHIDE THIN FILMS.....                                  | 42        |
| 4.4 METHODOLOGY FOR OPTICAL ABSORPTION MEASUREMENTS.....                            | 43        |
| 4.5 METHODOLOGY FOR X-RAY DIFFRACTION.....  | 43        |
| <b>CHAPTER FIVE.....</b>  | <b>44</b> |
| 5.0 RESULTS AND DISCUSSION.....   | 44        |

|  |           |
|--|-----------|
| 5.1 COPPER SULPHIDE (Cu <sub>x</sub> S)..... | 44        |
| 5.1.1 OPTICAL ABSORPTION.....                | 44        |
| 5.1.2 X-RAY DIFFRACTION .....                | 46        |
| 5.2 COPPER SELENIDE .....                    | 48        |
| 5.2.1 OPTICAL ABSORPTION.....                | 48        |
| 5.2.2 X-RAY DIFFRACTION .....                | 51        |
| <b>CHAPTER SIX .....</b>                     | <b>54</b> |
| 6.0 CONCLUSIONS AND RECOMMENDATION .....     | 54        |
| 6.1. CONCLUSIONS.....                        | 54        |
| 6.2 RECOMMENDATIONS .....                    | 55        |
| <b>REFERENCES.....</b>                       | <b>56</b> |



## LIST OF TABLES

|   |    |
|---|----|
| Table 5.1. Summary of the structural properties and score of as-deposited copper sulphide samples. .... | 47 |
| Table 5.2. Summary of the structural properties and score of annealed copper sulfide samples. ....      | 48 |
| Table 5.3: Summary of the structural properties and score of as-deposited copper selenide sample. ....  | 52 |
| Table 5.4: Summary of structural properties and score of annealed copper selenide samples. ....         | 53 |



## LIST OF FIGURES

|   |    |
|---|----|
| Figure 1.2: Crystal structure of a Covellite phase .....  | 4  |
| Figure 1.3: Crystal structure of $\text{Cu}_2\text{Se}$ phase of copper selenide .....  | 6  |
| Figure 2.1: Schematic of a CVD process.....   | 11 |
| Figure 2.2: Schematic of a SILAR process, (a) cationic precursor, (b) Ion exchange water, (c) Anionic precursor and (d) Ion exchange water. (Asim et al., 2014). .....                                | 12 |
| Figure 2.3. Diagram of a typical chemical bath deposition method (Musembi et al., 2013). .....  | 13 |
| Figure 2.4. Diagram of an electrophoretic deposition method. ....   | 13 |
| Figure 2.5. Schematic of a typical sputtering deposition method .....   | 14 |
| Figure 3.1 Energy band structures of conductors, semiconductors and insulators. ....  | 21 |
| Figure 3.2: Crystal structure of (a) crystalline, (b) polycrystalline and (c) amorphous semiconductors .....  | 22 |
| Figure 3.3: (a) DOS of a crystalline semiconductor; (b) DOS models proposed by Mott, (c) DOS models proposed by Cohen, Fritzsche and Ovshinski, and (d) DOS models proposed by Marshall and Owen..... | 24 |
| Figure 3.4: Schematic diagram of Chemical Bath Deposition Technique (Musembi et al., 2013).....   | 29 |
| Figure 3.5: Absorption coefficient plotted as a function of the photon energy in a typical semiconductor to illustrate the various possible absorption processes (Singh, 2006). .....                 | 30 |
| Figure 3.6: Diagram of a direct band gap semiconductor .....  | 32 |
| Figure 3.7: Diagram of an indirect band gap semiconductor. ....   | 33 |
| Figure 3.8: Shows a plot of $(Ah\nu)^2$ against $h\nu$ as proposed by Stern (1963).....   | 36 |
| Figure 3.9: Illustration of Bragg's law of Diffraction .....  | 38 |
| Figure 3.10: Schematic Diagram for X-ray Diffraction.....   | 38 |
| Figure 3.11. Illustration of the Reflection and Transmission geometry .....   | 39 |
| Figure 3.12: Schematic diagram of the rotating crystal method of X-ray diffraction .....  | 40 |

Figure 4.1. Experimental set-up of a CBD .....42

Figure 5.1: A plot of Absorbance against Wavelength for as-deposited and annealed  $\text{Cu}_x\text{S}$  thin film at different temperatures. ....44

Figure 5.2: A plot of  $(Ah\nu)^2$  vs  $h\nu$  for as-deposited  $\text{Cu}_x\text{S}$  thin film .....45

Figure 5.3: A plot of  $(Ah\nu)^2$  vs  $h\nu$  for  $\text{Cu}_x\text{S}$  thin film annealed at 573 K .....46

Figure 5.4: A plot of  $(Ah\nu)^2$  vs  $h\nu$  for  $\text{Cu}_x\text{S}$  thin film annealed at 673 K .....46

Figure 5.5: XRD pattern of copper sulphide as-deposited sample .....46

Figure 5.6: XRD pattern of  $\text{Cu}_x\text{S}$  powder annealed at 673 K .....47

Figure 5.7: A plot of Absorbance against Wavelength for as-deposited and annealed  $\text{Cu}_{2-x}\text{Se}$  thin film at different temperatures. ....49

Figure 5.8: A plot of  $(Ah\nu)^2$  vs  $h\nu$  for as-deposited  $\text{Cu}_{2-x}\text{Se}$  thin film .....50

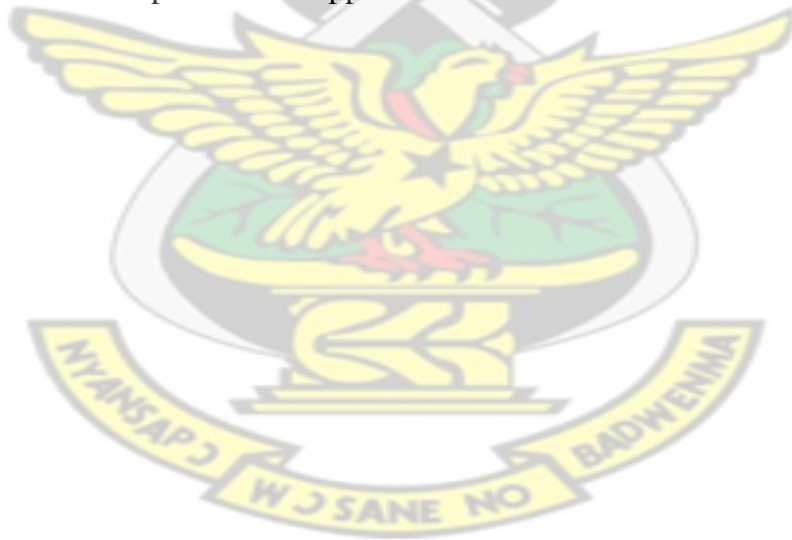
Figure 5.9: A plot of  $(Ah\nu)^2$  vs  $h\nu$  for  $\text{CuSe}$  thin film annealed at 473 K. ....50

Figure 5.10: A plot of  $(Ah\nu)^2$  vs  $h\nu$  for  $\text{CuSe}$  thin film annealed at 573 K .....50

Figure 5.11: A plot of  $(Ah\nu)^2$  vs  $h\nu$  for  $\text{CuSe}$  thin film annealed at 673 K .....50

Figure 5.12 XRD pattern of as-deposited Copper selenide .....51

Figure 5.13 XRD pattern of Copper selenide annealed at 673 K .....52



## LIST OF SYMBOLS AND ACRONYMS

A Absorbance

Å Armstrong

a-Si Amorphous Silicon

CBD Chemical Bath Deposition

CdS Cadmium sulphide

CdTe Cadmium Telluride

CIGS Copper Indium Gallium Selenide

COD Crystallography Open Database

c-Si Crystalline Silicon

Cu<sub>2-x</sub>Se, CuSe, Cu-Se Copper selenide

Cu<sub>x</sub>S Copper sulphide

CVD Chemical Vapour Deposition

D Crystalline size/ Grain size

DOS Density of states

E<sub>g</sub> Energy band gap

FWHM Full width at half maximum

GaAs Gallium Arsenide

*h* Plank constant

IP Ionic product

*k* Wave vector

K<sub>sp</sub> Solubility constant

PV Photovoltaic

PVD Physical Vapour Deposition

SILAR Successive Ionic Layer Adsorption and Reaction

UV Ultraviolet

$\nu$  Photon frequency

VIS Visible spectrum

XRD X-ray Diffraction

$\alpha$  Absorption coefficient

$\lambda$  X-ray wavelength

## CHAPTER ONE

### INTRODUCTION

Semiconducting materials play an important role in our modern day electronics. In the early days of radio and television, transmitting and receiving equipment relied on vacuum tubes, but these have been almost completely replaced in the last four decades by semiconducting materials, including transistors, diodes, integrated circuits and other solid-state devices (Young and Freedman, 2008). Such devices have found wide applications due to their numerous advantages such as compact sizes, reliability, power efficiency, and low cost. As discrete components, they have found use in power devices, optical sensors, and light emitters, including solid-state lasers. More importantly, they can be easily incorporated into easily manufacturable microelectronic circuits. They are, and will continue to be one key element for almost all electronic systems in the foreseeable future.

During the early 1950s, germanium was the major semiconductor material. However, it proved unsuitable for many applications, because devices made of the material exhibited high leakage currents at only moderately elevated temperatures. Hence the incorporation of silicon, which virtually replaced germanium as a material for device fabrication. The main reasons for this are twofold: (1) silicon devices exhibit much lower leakage currents, and (2) silicon dioxide ( $\text{SiO}_2$ ), which is a high-quality insulator, is easy to incorporate as part of a silicon-based device. Thus, silicon technology has become very advanced and invasive, with silicon devices constituting more than 95 percent of all semiconductor products sold worldwide.

Compound semiconductors have been a subject of semiconductor research for nearly as long as elemental semiconductors such as silicon and germanium. Compound

semiconductors, whose merit of superior transport was recognized as early as 1952 by Welker, have continued to be of interest although their success has been narrower in scope. The areas of significant applications include light sources (light emitting diodes and light amplification by stimulated emission of radiation), microwave sources (Gunn diodes, Impatt diodes, etc.), microwave detectors (metal-semiconductor diodes, etc.), and infrared detectors. All of these applications have been areas of the semiconductor endeavour to which compound semiconductors are uniquely suited. Compound semiconductors have also made significant contributions to the generation of electricity from solar radiation. Today's most efficient technology for the generation of electricity from solar radiation is the use of multi-junction solar cells made of III-V compound semiconductors. Efficiencies up to 39 % have already been reported under concentrated sunlight. These solar cells have initially been developed for powering satellites in space and are now starting to explore the terrestrial energy market through the use of photovoltaic concentrator systems. This opens a huge potential market for the application of compound semiconductor materials due to the large areas that are necessary to harvest sufficient amounts of energy from the sun. Concentrator systems using III-V solar cells have shown to be ecological and could play an important role for the sustainable energy generation of the future (Dimroth, 2006).

Extensive research has been devoted to grow various kinds of binary and ternary semiconductor thin films (Bedir *et al.*, 2005). This is due to their potential applications in the area of solar cells, optoelectronic devices, photoconductors, sensors, thin films polarizers, thermoelectric cooling materials and infrared detector devices. Two of such binary semiconductor thin films are copper sulphide ( $\text{Cu}_x\text{S}$ ) and copper selenide ( $\text{Cu}_{2-x}\text{Se}$ ).

## 1.1 COPPER SULPHIDE

Copper sulphide is an important semiconducting material because of its use mainly in photovoltaic. It appears in the colour range of dark gray to indigo to blue- black. Its band gap in the bulk is 1.21 eV and a melting and boiling point of 103 °C and 220 °C respectively. At least five stable phases of the copper sulphide system are known to exist naturally. Among the  $\text{Cu}_x\text{S}$  ( $1 \leq x \leq 2$ ) phases include: covellite ( $\text{Cu}_{1.00}\text{S}$ ), anilite ( $\text{Cu}_{1.7}\text{S}$ ), digenite ( $\text{Cu}_{1.80}\text{S}$ ), djurleite ( $\text{Cu}_{1.97}\text{S}$ ), and chalcocite ( $\text{Cu}_{2.00}\text{S}$ ) (Pathan and Lokhande, 2004; Evans, 1981).

Figure 1.1 and 1.2 shows the crystal structure of chalcocite and covellite phases of copper sulphide respectively.

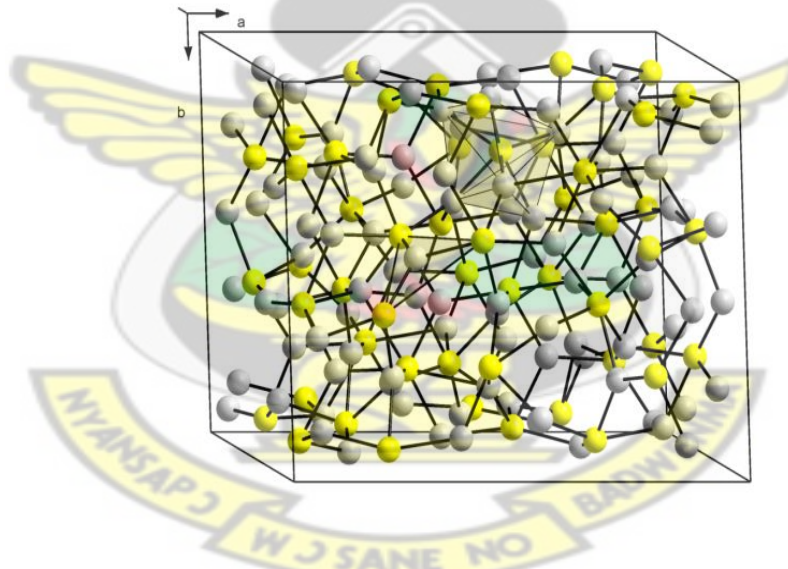


Figure 1.1: Crystal structure of Chalcocite

([en.m.wikipedia.org/wiki/file:Kristallstruktur\\_Chalkosin](https://en.m.wikipedia.org/wiki/file:Kristallstruktur_Chalkosin))

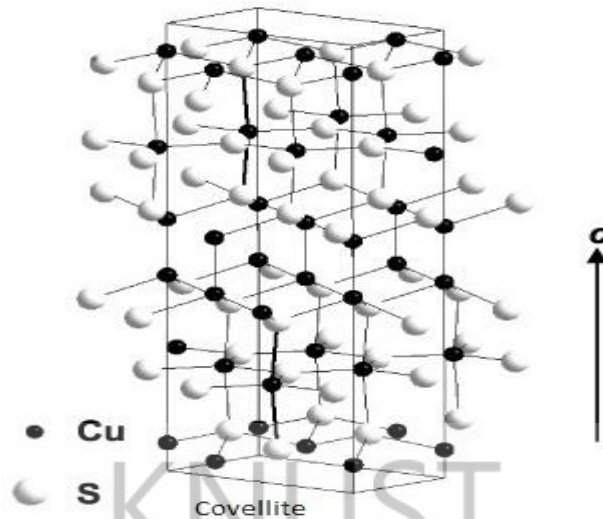


Figure 1.2: Crystal structure of a Covellite phase

(ej.iop.org)

Other phases that exist include yarrowite ( $\text{Cu}_{1.12}\text{S}$ ) and spionkopite ( $\text{Cu}_{1.14}\text{S}$ ) (Goble, 1985). The structure of chalcocite and djurleite is hexagonal with alternate layers of copper and sulphur ions. The covellite contains 6 formula units in the unit cell with four copper ions tetrahedrally coordinated and two triangular coordinates with a hexagonal crystal structure. (Wyckoff, 1965; Evans, 1981)

Among the group I-VI compounds, copper sulphide thin films are used in photovoltaic and various optoelectronic devices (Ali *et al.*, 1995). Its use in combination with CdS as a solar cell material was massively investigated between the 1960s and 1980s. (Rothwarf and Barnett, 1977). In thin film studies,  $\text{Cu}_2\text{S}/\text{CdS}$  solar cells showed significant promise, but the diffusion and doping of copper into the CdS layer led to long-term performance degradation and ultimately an abandonment of this system. With the advent of nano-crystal-based methods, which tend to use much milder processing conditions, and in which diffusion and doping issues take on entirely new behaviour, it is worthwhile to re-examine this material combination. (Yue *et al.*, 2008)

The preparation of thin films of  $\text{Cu}_x\text{S}$  has been explored by a number of methods including solid state reaction (Parkin, 1996), chemical vapour deposition (Scheider *et al.*, 2007), spray pyrolysis (Isac *et al.*, 2007), chemical bath deposition (Bagul *et al.*, 2007; Chen *et al.*, 2008; Bini *et al.*, 2000; Munce *et al.*, 2007; Ilenikhena, 2008; Offiah *et al.*, 2012; Kumar *et al.*, 2013) and SILAR (Pathan *et al.*, 2002; Wang *et al.*, 2009).

## 1.2. COPPER SELENIDE

Copper selenide ( $\text{Cu}_{2-x}\text{Se}$ ), has also recently generated a lot of interest since it has been widely used as a solar cell (Lakshmikumar, 1994). Copper selenide is a metal chalcogenide which has colour ranging from blue-black to bluish green depending on the type of stoichiometric composition. The band gap of copper selenide is not well defined because of the wide variety of stoichiometric forms. Herman *et al.* (1983) reported a direct and indirect band gap of 2.2 eV and 1.4 eV respectively and also Murali *et al.* (2009) reported a band gap of 2.18 eV. It has a melting point of  $550^\circ\text{C}$  ([www.webelements.com](http://www.webelements.com)). Its indirect band gap is near the optimum value for solar cell applications and hence could offer a high efficiency of conversion of up to 8.8 % (Chopra *et al.*, 1983). Copper selenide is a semiconductor with p-type conductivity. The attraction of this material also lies in the feasibility of producing the ternary material,  $\text{CuInSe}_2$  (Chu *et al.*, 1984; O'Brien and Santhanam, 1992) and also as an important surface impurity in Cu-rich  $\text{CuInSe}_2$  (Fons *et al.*, 1998). Depending on the method of fabrication, copper selenide exists in different crystallographic forms at room temperature. It exists in the cubic, tetragonal or orthorhombic or monoclinic forms (Toneje and Toneje, 1981; Kashida and Akai, 1988; Haram *et al.*, 1992; Levy-Clement *et al.*, 1997).  $\text{Cu}_{2-x}\text{Se}$  is known to have five stable phases;  $\alpha\text{-Cu}_2\text{Se}$  (Bellidoite),  $\text{Cu}_3\text{Se}_2$  (umangite),  $\text{CuSe}$  (Klockmannite),

CuSe<sub>2</sub> (Krutaite), Cu<sub>2-x</sub>Se (berzelianite). Figure 1.3 shows the Cu<sub>2</sub>Se phase of copper selenide.

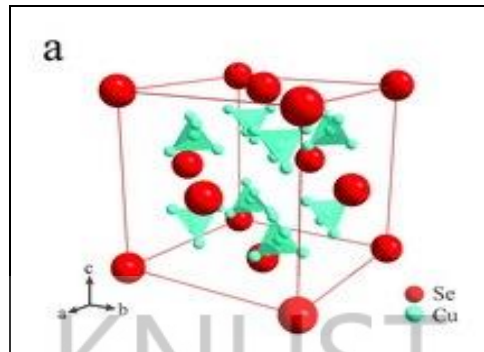


**Figure 1.3: Crystal structure of Cu<sub>2</sub>Se phase of copper selenide**  
(www.nature.com)

The thermal stability of these compounds varies greatly depending on the composition. It is also reported that CuSe has a hexagonal structure at room temperature and undergoes transition to an orthorhombic structure at 48 °C and back to a hexagonal structure at 120 °C (Haram *et al.*, 1992; Garcia *et al.*, 1999; Lakshmi *et al.*, 2001). A face centered cubic structure is reported for Cu<sub>2-x</sub>Se with  $0.15 \leq x \leq 0.2$  at room temperature, and eventually it will attain the tetragonal structure of Cu<sub>2</sub>Se phase (Garcia, 1999). A wide variety of deposition techniques have been employed for depositing Cu<sub>2-x</sub>Se thin films such as vacuum evaporation (Hermann and Fabick, 1983; Chopra and Das, 1983), electro-deposition (Massaccesi *et al.*, 1993; Haram and Santhanam, 1994), chemical bath deposition (CBD) (Okereke *et al.*, 2011; Khomane, 2012), electrophoretic deposition (Razak and Sharin, 2007), brush electroplating and SILAR method (Murali *et al.*, 2009; Pathan *et al.*, 2004).

### 1.3 OBJECTIVE OF THE PROJECT

Recently, thin films of copper sulphide and copper selenide have become of great interest to the photovoltaic industry. This is as a result of their properties. One of such properties is their variable band gap which can be adjusted to the ideal band gap

of solar cells.  $\text{Cu}_x\text{S}$  and Cu-Se thin films are known to produce a high conversion efficiency of about 8.8 % hence can be used in photovoltaics (Garcia, 1999). Many deposition techniques have been employed in the preparation of these films but one very promising technique is the chemical bath deposition technique. This technique possesses many advantages over the others such as its non-sophisticated instrumentation, convenience for large area deposition of substrates of different materials and generally very simple.

### **1.3.1. SPECIFIC OBJECTIVES**

The research presented in this thesis was motivated by the following objectives:

- To deposit  $\text{Cu}_x\text{S}$  and Cu-Se thin films using the chemical bath technique.
- To investigate the optical band gap using optical absorption spectroscopy.
- To investigate the structure and composition of the thin films using the powder x-ray diffraction analysis.
- To investigate the effect of annealing on the optical and structural properties of the thin films.

### **1.4. REASONS FOR INVESTIGATING THE OPTICAL PROPERTIES, CRYSTAL STRUCTURE OF THE THIN FILM AND THE EFFECT OF ANNEALING.**

Experimental investigations on the optical behavior of thin films deal primarily with optical reflection, transmission and absorption properties, and their relation to the optical constants. Optical properties are directly related to the structural and electronic properties of solids, and hence very important in device applications. A detailed knowledge of optical properties can provide a huge amount of information about their structure, optoelectronic behavior, transport of charged carriers, etc.

(Singh and Shimakawa, 2003). These properties determine whether a semiconductor will serve well in a specific application. An investigation into the crystal structure will help in the determination of the crystallographic parameters such as the average grain size, phase, composition and the preferred orientation. These are important parameters for device application. XRD patterns also serve as a ‘fingerprint’ to confirm the compound deposited.

Annealing of semiconductor surfaces plays an important role in the crystallization process of the semiconductor crystal. It enhances the crystals quality, performance and reliability. Annealing also reduces defects, and lowers surface roughness (Zinoviev *et al.*, 2001). Being able to ‘tune’ the optical properties through annealing can result in materials for specific applications.

#### **1.4.1. JUSTIFICATION OF THE PROJECT**

Sunlight is by far the most abundant form of renewable energy. However, harnessing this energy is still too expensive. We are in a country where there is abundance of sunlight yet we are still in a terrible state of energy crisis. In view of this, there is the need to resort to other alternative means of power generation and one laudable form is solar energy. The demand for clean energy has spurred academic interest in new and efficient ways to capture and store sunlight. Harnessing this energy will require the use of suitable semiconducting thin film materials and two of such promising materials are Copper Sulphide and Copper Selenide.

Another motivation for this project is the need for non-toxic, inexpensive and abundant semiconducting materials that can be used in Photovoltaic (PV). The current Photovoltaic materials experience certain drawbacks. Examples of some of such PVs are:

- ❖ c-Si---Requires thick layers which increases cost
- ❖ a-Si---Low mobility, stability problems
- ❖ GaAs---Arsenic toxicity, substrate cost
- ❖ CIGS---Indium scarcity/cost
- ❖ CdTe---Cadmium toxicity, tellurium scarcity/cost

## 1.5. STRUCTURE OF THE THESIS

The thesis is in six chapters: Chapter One gives an introduction to the importance of semiconductor research over the years and some properties of  $\text{Cu}_x\text{S}$  and Cu-Se thin films. It also talks about the objectives, justification and the reasons for interest in semiconducting materials such as  $\text{Cu}_x\text{S}$  and Cu-Se. The Second chapter deals with the literature review; the various thin film deposition techniques are discussed in detail. This chapter also reviews literature on the deposition of  $\text{Cu}_x\text{S}$  and Cu-Se thin films by chemical bath deposition technique. Chapter Three treats the relevant theory governing this research. The methods and materials, post-deposition treatment used in this research are presented in Chapter Four. Chapter Five then deals with the results in graphical representation coupled with an in-depth discussion of the results. This is followed by Chapter Six with conclusion and recommendation.

## CHAPTER TWO

### 2.0 LITERATURE REVIEW

#### 2.1. THIN FILM TECHNOLOGY

Thin film is a layer of material ranging from fractions of a nanometer to several micrometers. The act of applying or depositing a thin film onto a surface or substrate is termed thin film deposition. “Thin” is a relative term, but most of the deposition techniques control the layer thickness within a few tens of nanometers ([www.wikipedia.com](http://www.wikipedia.com)). In recent times, the study of bulk semiconductors have been replaced with that of thin films due to the fact that thin films have mechanical, electrical, magnetic and optical properties which may differ from those of the bulk material and are used commonly in the form of a deposit on a suitable substrate for integrated circuit, resistors, capacitors, transistors and superconductors just to mention a few (Thewlis, 1979). The usefulness of the optical properties of thin films and the scientific curiosity about the behavior of two dimensional solids has been responsible for the immense interest in the study of science and technology of thin films. The technology and understanding of films less than 1 micron thick have made tremendous advances in the last 50 to 60 years basically because of industrial demand for reliable thin film microelectronics devices (Nadeem *et al.*, 2005).

##### 2.1.1. TYPES OF THIN FILM DEPOSITION TECHNIQUES

In the past few decades, several deposition techniques such as chemical bath deposition, vacuum evaporation, electro-deposition, molecular beam epitaxy, close speed sublimation, thermal evaporation, spray pyrolysis, sputter deposition, etc. , have been used in the deposition of thin films. Literature shows that, Bunsen and

Grove firstly obtained metal films in 1852 by means of chemical deposition and flow discharge of sputtering. Faraday made metal films in 1857 by the thermal evaporation on explosion of a current carrying metal wire (Nadeem *et al.*, 2005). In addition to a variety of new and future based technology, thin films studies have directly and indirectly progressed in many new areas of research in solid state physics and chemistry which are based on phenomena uniquely characteristic of thickness, geometry and structure of films. Depending on the type of material, various deposition methods can be employed.

**2.1.1.1. Chemical vapour deposition (CVD)** is a chemical process for depositing thin films of various materials. In a typical CVD process, the substrate is exposed to one or more volatile precursors, which react and/or decompose on the substrate surface to produce the desired deposit. Frequently, volatile by-products are also produced, which are removed by a gas flow through the reaction chamber. Figure 2.1 describes the CVD process.

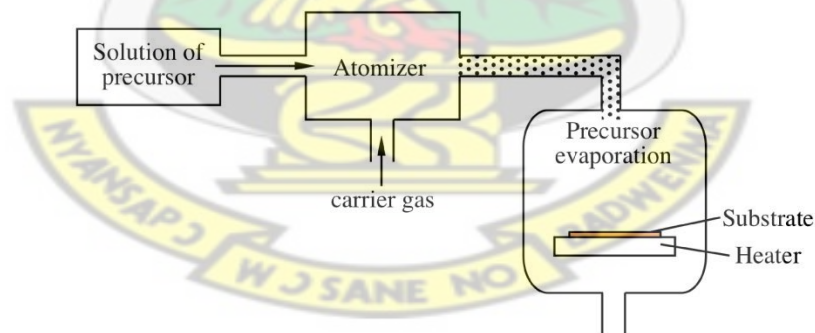


**Figure 2.1: Schematic of a CVD process**  
([www.precisionfab.net](http://www.precisionfab.net))

**2.1.1.2. SILAR method (Successive Ionic Layer Adsorption and Reaction):** The SILAR method is used to create coatings on thin films for technological products such as photovoltaic cells that convert sunlight into energy for use in solar power

applications. By allowing thin films to be coated in different chemicals at or close to room temperature, metallic films or films incorporating metallic parts can use the SILAR method and avoid possible problems with damage caused by oxidation or corrosion. SILAR requires the film to be immersed in the chemicals required for creating a chemical solution over the substrate. Between each immersion of the film into the chemicals, the film is rinsed using purified water to create the desired coating over the film. A schematic illustration can be seen in figure 2.2.

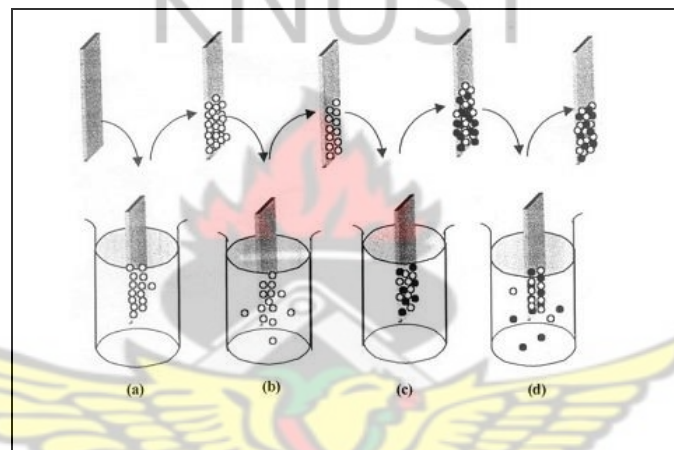


**Figure 2.2: Schematic of a SILAR process, (a) cationic precursor, (b) Ion exchange water, (c) Anionic precursor and (d) Ion exchange water. (Asim et al., 2014).**

**2.1.1.3. Chemical bath deposition (CBD):** Chemical bath deposition (CBD) is becoming an important deposition technique for thin films of compound materials like chalcogenides (Hodes, 2002). A major success can be found in the recent period with the deposition of semiconducting cadmium sulphide, or zinc sulphide or window layer, in efficient copper indium diselenide or cadmium telluride thin film solar cells. CBD takes advantage of the use of a reaction from a solution where different precursors can be dissolved easily either in the ionic or molecular form and react chemically on the substrates leading to film formation. The key advantages are

low cost, large area and low temperature atmospheric processing (Lincot *et al.*, 1999). This technique is a relatively inexpensive, simple thin film process that is able to produce uniformly large area deposition. An illustration of this technique is shown in figure 2.3

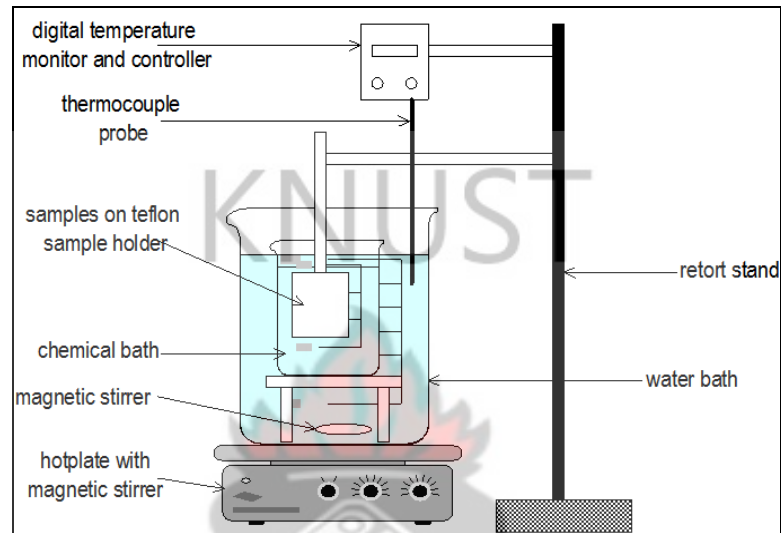


**Figure 2.3. Diagram of a typical chemical bath deposition method (Musembi et al., 2013).**

#### 2.1.1.4. Electrophoretic deposition:

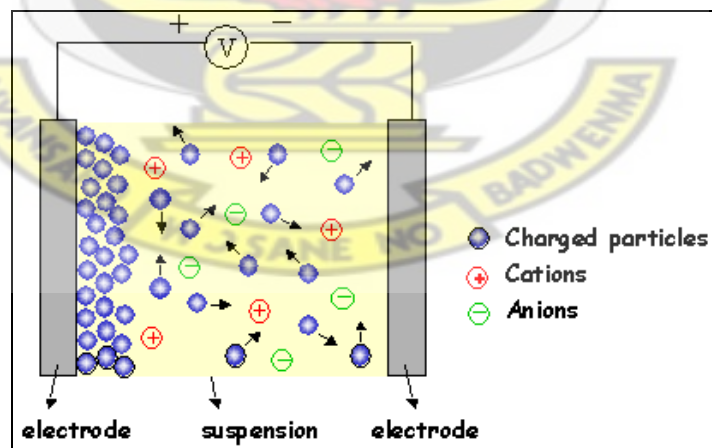


**Figure 2.4. Diagram of an electrophoretic deposition method. (www.mtm.kuleuven.be)**

Figure 2.4 describes the electrophoretic method. This is a rapid two-step process whereby the first step involves the particles acquiring an electric charge in the liquid

in which they are suspended. The particles are forced to move towards one of the electrodes by applying an electric field to the suspension. In the second step, the particles collect at one of the electrodes and form a consistent deposit on it. The deposit takes the shape imposed by this electrode.

#### 2.1.1.5. Sputtering:

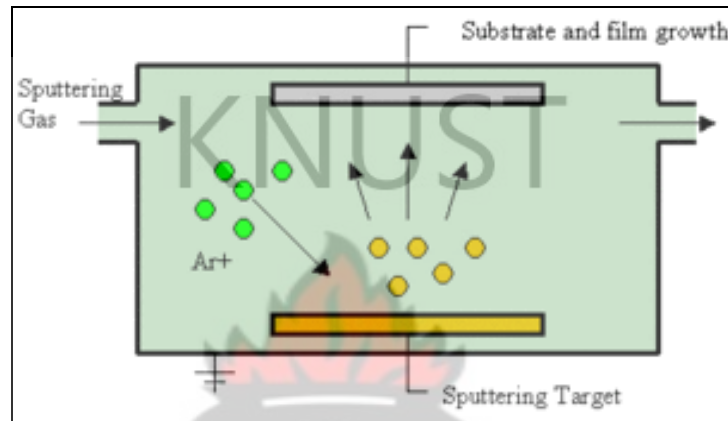


**Figure 2.5. Schematic of a typical sputtering deposition method**  
([en.wikipedia.org/wiki/Sputter\\_deposition](http://en.wikipedia.org/wiki/Sputter_deposition))

This is a physical vapor deposition (PVD) method of depositing thin films. This involves ejecting a material from a target that is a source onto a substrate such as a silicon wafer. Sputtered ions ballistically fly from the target in straight lines and impact energetically on the substrates or vacuum chamber. Alternatively, at higher pressures, the ions collide with the gas atoms that act as a moderator and move diffusely, reaching the substrates or vacuum chamber wall and condensing after undergoing a random walk. The sputtering gas is often an inert gas such as argon which is not always readily available. Figure 2.5 shows the PVD process.

Thin films prepared by chemical methods are generally less expensive than those prepared by other cost intensive techniques. The chemical bath deposition method due to its many advantages like low cost, large area production and simplicity in

instrumental operation is employed in this particular experiment. It may allow us to easily control the growth factors such as film thickness, deposition rate and quality of crystallites by varying the solution pH, temperature and bath concentration (Sankapal *et al.*, 2004).

## **2.2. REVIEW OF COPPER SULPHIDE THIN FILMS DEPOSITED BY CHEMICAL BATH TECHNIQUE**

Since the discovery of photovoltaic effect in CdS/Cu<sub>x</sub>S structure in the mid-fifties, there has been widespread interest in Cu<sub>x</sub>S thin films. Various methods such as evaporation, reactive sputtering and improved topotaxial reaction have been used to obtain Cu<sub>x</sub>S films with  $x \sim 1.997$  as required for solar cell applications (Vucic *et al.*, 1984). In recent years this material is pursued for its solar control application (Heyding, 1966; Toneje and Toneje, 1981). Many researchers have reported on chemical bath deposition of Cu<sub>x</sub>S.

Fatas *et al.* (1985) mixed 1 M CuSO<sub>4</sub>, 1 M sodium acetate and 7.4 M TEA solution and then added 1M thiourea in an alkaline medium. They reported an optical band gap of 2.58 eV and resistivity of the order of  $3 \times 10^{-3} \Omega \text{ cm}$ .

Varkey (1989) reported Cu<sub>x</sub>S deposition using EDTA as a complexing agent in a bath comprising of CuCl<sub>2</sub>, NaCl and hydroxylamine hydrochloride solutions. Gadave *et al.* (1993) did this in a different way. An aqueous solution of 15 ml 0.1 M CuSO<sub>4</sub> and 15 ml 1 M sodium thiosulfate was mixed and clean glass slides were introduced in this reaction bath of pH 0.5 for a duration of 40 minutes. The temperature of deposition was 60 °C. This resulted in Cu<sub>x</sub>S films of band gap 2.4 eV and electrical resistivity of the order of  $10^{-4} \Omega \text{ cm}$ .

Ilenikhena (2008) deposited  $\text{Cu}_x\text{S}$  thin films by improved chemical bath method with starting chemicals of  $\text{CuCl}_2 \cdot 2\text{H}_2\text{O}$ ,  $\text{NH}_3$  and EDTA as a complexing agent and thiourea as the source of sulphur ion. They reported a band gap of  $(2.10 - 2.35) \pm 0.05$  eV. Observations made in this research showed that copper sulphide ( $\text{CuS}$ ) thin film deposited at a pH of 7 had the lowest absorbance within the wavelength range of 350 nm to 900 nm while the films deposited at a pH of 12 had the highest absorbance.

Offiah *et al.* (2012) investigated the structural and spectral properties of chemical bath deposited  $\text{Cu}_x\text{S}$ . The article reported an optical band gap of 2.4 eV (direct) and 1.0 - 1.4 eV (Indirect) using starting reagents of 1M  $\text{CuCl}_2 \cdot 2\text{H}_2\text{O}$ , thiourea, 25 % ammonium solution and triethanolamine (TEA) ( $\text{N}(\text{CH}_2\text{CH}_2\text{OH})_3$ ). They reported that the thermally treated  $\text{Cu}_x\text{S}$  thin films (300 °C and 400 °C) were observed to have very high transmittance, between 85 % and 95 %, in both the visible and the NIR region of the electromagnetic spectrum. They concluded that the high transmittance and low reflectance properties of the  $\text{Cu}_x\text{S}$  thin films annealed at 300 °C and 400 °C make them good material for anti-reflection coatings which could as well be employed in solar thermal and other optical devices to reduce solar reflectance and enhance their transmittance. The observed XRD patterns for the as-deposited copper sulphide thin film showed that the films had a structure that matched well with the mineral chalcocite with corresponding diffraction ( $2\theta$  peak) angles of  $31.94^\circ$  and  $70.77^\circ$  and (h k l) planes being (0 0 4) and (1 0 8). The XRD pattern for the copper sulphide thin films annealed at 400 °C compared very well with that of the compound, digenite. The samples annealed at 400 °C showed diffraction angles at  $26.29^\circ$ ,  $29.31^\circ$ ,  $32.20^\circ$  and  $40.07^\circ$  with corresponding (h k l) planes as (1 0 1), (1 0 7), (1 0 10) and (1 0 16).

Santos *et al.* (2012) also prepared  $\text{Cu}_x\text{S}$  thin films using the chemical bath method. The glass slides were immersed vertically in an aqueous solution containing copper sulphate ( $\text{CuSO}_4 \cdot 5\text{H}_2\text{O}$ ), sodium acetate ( $\text{NaCOOH}$ ), triethanolamine ( $(\text{HOCH}_2\text{CH}_2)_3\text{N}$ ), and thiourea ( $\text{CH}_4\text{N}_2\text{S}$ ). A reported band gap within the range of 1.8 eV to 2.4 eV and an increased transmittance with increasing annealing temperatures were observed.

Recently, Singh *et al.* (2013) synthesized CuS thin films using chemical bath deposition. Starting reagents of 0.1 M (Copper sulphate, tartaric acid, thiourea and ammonia) were used. A reported optical band gap within a range of 1.2 to 3.0 eV and an XRD analysis revealed a hexagonal covellite CuS crystal structure.

Adel and Mustafa (2013) also investigated the effect of annealing on the structural and optical properties of CuS thin film prepared by chemical bath deposition (CBD). They used copper sulfate, thiourea, triethanolamine (TEA) and ammonia as reagents for the experiment. A reported band gap within the range of 2.4 eV to 2.5 eV was observed, the optical transmittance of CuS thin film decreased with increasing concentration of Cu in the bath solutions and the transmittance increased after annealing process. They concluded that the films could be used as transparent conducting materials (TCM) which is widely used as electrodes in solar cells and flat-panel displays.

### **2.3. REVIEW OF COPPER SELENIDE THIN FILMS DEPOSITED BY CHEMICAL BATH TECHNIQUE**

Several deposition techniques have been used for the growth of copper selenide thin films such as solution growth technique (Gosavi *et al.*, 2008), successive ionic layer adsorption reaction (SILAR) (Pathan *et al.*, 2004), sol-gel method (Gurin *et al.*,

2008), brush electroplating (Murali and John, 2009), electrochemical (Jagminas *et al.*, 2006), modified chemical deposition (Pathan *et al.*, 2003), chemical precipitation and dip coating (Zainal *et al.*, 2005) and chemical bath deposition (Al- Mamum *et al.*, 2005; Bhuse *et al.*, 2003). In recent research, the chemical bath deposition technique has been employed due to its many advantages over the others.

Garcia *et al.* (1999) published an article on the effect of thermal processing on optical and electrical properties of copper selenide thin films using CBD. This paper reported low crystallinity in the as-prepared copper selenide thin films whereas annealing the film in nitrogen enhanced the crystallinity. A hexagonal phase was also reported after structural analysis was performed. A decrease in the electrical conductivity with annealing temperature was also reported.

Similarly, using the chemical bath deposition technique, Bahri *et al.* (2008) investigated the structural, optical and electrical properties of  $\text{Cu}_{2-x}\text{Se}$  thin films with starting chemicals of cupric chloride, sodium selenosulphate and ammonia to adjust the pH. The deposition was performed for 2 hours. They reported an optical band gap within the range of 2.11 to 2.51 eV and peak positions which correspond to reflections from the (1 1 1), (0 2 2), (1 1 3) and (0 0 4) planes of the cubic phase. An increase in conductivity with increasing temperature was observed.

Okereke and Ekpunobi (2011), also reported an optical band gap of 2.0 - 2.3 eV (direct) and 0.4-0.8 eV (Indirect) using CBD. Their starting reagents were copper tetraoxosulphate (VI), selenium trioxosulphate (V), sodium thiosulphate and ammonia. The bath was kept at room temperature. Peak positions corresponding to reflections from the (1 1 0), (2 0 0), (2 1 0), (0 1 2), (1 3 0), (3 1 0), (0 4 0) and (4 1 1) planes of the monoclinic phase was reported.

Khomane (2012) published an article on the synthesis and characterization of chemically deposited  $\text{Cu}_{2-x}\text{Se}$  thin films. The starting reagents used were copper sulphate dihydrate, maleic acid and sodium selenosulphate. A band gap of 2.20 eV was reported and he concluded that it was useful in the fabrication of hetero-junction solar cells. A cubic crystal phase was also reported. The resistivity of the sample decreased with increase in temperature which indicated the semiconducting nature of the sample. The film sample showed high electrical conductivity and he concluded that the films could be used as radiation filters.

Durdu *et al.* (2013) presented an article on the investigation of zinc selenide and copper selenide thin films produced by chemical bath deposition. In this article, the deposition bath for copper selenide thin film consisted of an aqueous solution of 4 ml (0.5 M) copper sulphate pentahydrate ( $\text{CuSO}_4 \cdot 5\text{H}_2\text{O}$ ), 4 ml (0.1 M) trisodium citrate, 1 ml (0.5 M) sodium hydroxide, and 4 ml sodium selenosulphate ( $\text{Na}_2\text{SeSO}_3$ ) solution. The XRD pattern reported showed that  $\text{Cu}_3\text{Se}_2$  films had a tetragonal structure known as umangite.

## CHAPTER THREE

### 3.0. THEORETICAL BACKGROUND

#### 3.1. SEMICONDUCTORS

Solids are primarily classified as insulators, metals and semiconductors. Semiconductors are materials that have conductivities between conductors (high conductivity) and insulators (no conductivity), conductivity roughly in the range of  $10^3$  to  $10^{-8}$  siemens per centimeter.

##### 3.1.1. BASIC SEMICONDUCTOR CONCEPT

The concept of “energy bands” is very useful in classifying materials as insulators, semiconductors and conductors. The energy band diagram is a representation of the different allowed and available energy levels which an electron can occupy. The most important concept in the energy band diagram is the shape of the bands and their mutual energy separation. When similar atoms are brought close enough to each other to form a solid, the independent degenerate wave functions of their electrons overlap and as a way to satisfy the Pauli’s exclusion principle (no two electrons can occupy the same quantum state), this degeneracy splits and the corresponding energy levels spread into a continuous range of energy levels instead of discrete levels in an isolated atom called the energy band. There may (as in insulators and semiconductors) or may not (as in metals) exist an *energy gap* (forbidden band) between bands as shown in figure 3.1, depending on a number of factors, including the type of atom(s) in the solid, lattice structure and temperature. The band gap in insulators may be as wide as 6 eV. In semiconductors, the

conduction band is separated from the valence band usually by a narrow band gap of about  $1\text{ eV}$ . In metals, the conduction band overlaps the valence band.

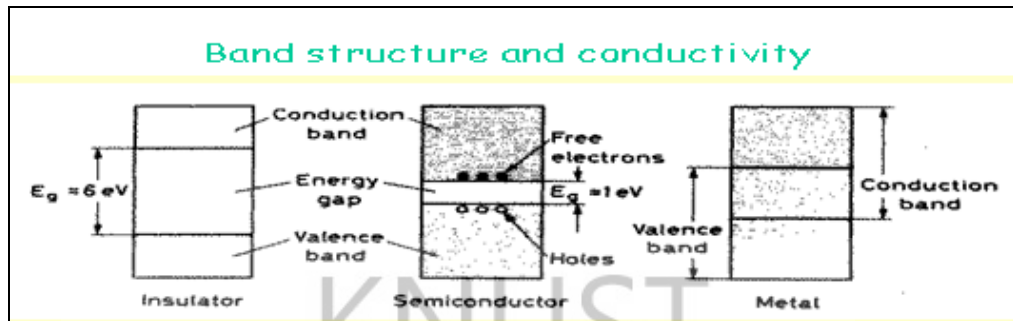


Figure 3.1 Energy band structures of conductors, semiconductors and insulators.

### 3.1.1.1. CONDUCTIVITY IN SEMICONDUCTORS.

The band structure of semiconductors is such that at absolute zero, the valence band is completely filled (all atoms are in the ground state) and the conduction band is completely empty. If a voltage is applied, there is no conduction of electrons because there are no empty spaces to allow the electrons to move around. In order for conduction to occur, electrons must be excited to the next higher band, known as the conduction band. In semiconductors, the conduction band is normally empty at absolute zero but is separated from the valence band by only a small amount of energy gap of about  $0.1$  to  $1\text{ eV}$ . Valence electrons can overcome this barrier by absorbing a small amount of energy from thermal or optical sources. This then creates a free electron in the conduction band and a hole (missing electron) in the valence band.

Conductivity in semiconductors is also affected by temperature. As temperature is increased, some electrons gain sufficient amount of energy and move across the gap into the conduction band where they can move freely and conduct when a field is

applied. Thus conductivity of semiconductors is said to be greatly dependent on the band gap and temperature. Within certain limits, higher temperatures gives rise to high electron concentration in the conduction band resulting in higher conductivity and an equal number of unoccupied states called holes in the valence band.

### 3.1.2. CLASSIFICATION OF SEMICONDUCTORS

There are several ways of classifying semiconductors and one important division is into crystalline, polycrystalline and amorphous. Each type is characterized by the size of an ordered region within the material. An ordered region is spatial volume in which atoms or molecules have a regular geometric arrangement or periodicity (Neamen, 2003). Figure 3.2 shows the three types of semiconducting materials.

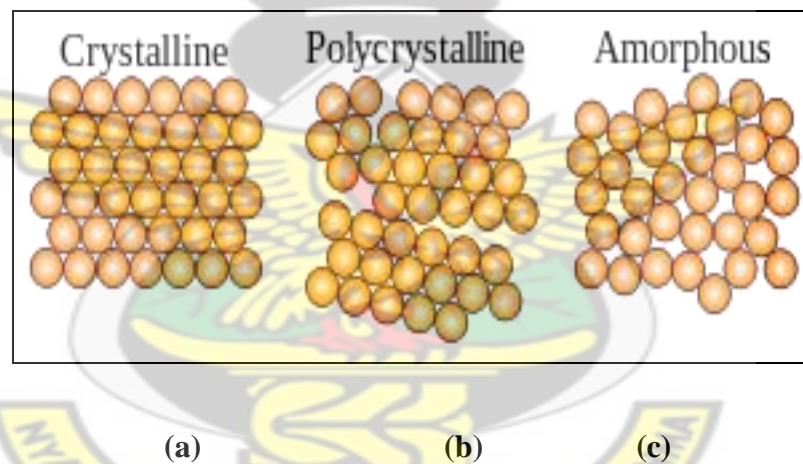


**Figure 3.2: Crystal structure of (a) crystalline, (b) polycrystalline and (c) amorphous semiconductors ([www.answers.com/topic/crystal](http://www.answers.com/topic/crystal)).**

#### 3.1.2.1. CRYSTALLINE SEMICONDUCTORS

A crystalline material consists of atoms that are arranged in a periodic, regularly repeated three dimensional pattern. In crystalline materials, a radial distribution function exhibits series of sharp peaks indicative of the long-range order. The electronic band structure in these materials have periodicity of the atomic structure, and the presence of long-range order results in a band structure with allowed and

forbidden electronic levels, with sharp band edges and a fundamental energy gap separating valence band from conduction band. (Yacobi, 2003)

### **3.1.2.2. POLYCRYSTALLINE SEMICONDUCTOR**

A polycrystalline material consists of crystal grains that are randomly oriented with respect to each other. Between two grains, a grain boundary exists. An important parameter is the grain size and its distribution. Polycrystalline semiconductors are used in cheap, large –area applications such as solar cells or thin- film transistors. Polycrystalline material can be fabricated from an amorphous material using annealing procedures (Grundmann, 2006).

### **3.1.2.3. AMORPHOUS SEMICONDUCTORS**

An amorphous solid is any non-crystalline solid in which the atoms and molecules are not organized in a definite lattice pattern or a solid whose atomic structure is random such that long range atomic order is absent. According to Grundmann (2006), amorphous solids, nevertheless, retain the short range order due to valence bonding of atoms, which is also characteristic of crystalline solids. The short-range order is responsible for the observation of semiconductor properties such as an optical absorption edge and also thermally activated conductivity. Amorphous materials can be re-crystallized into polycrystalline materials upon annealing. The number of nearest neighbors to any atom is not much different from the corresponding number in the crystalline material (Yacobi, 2003). Bonding angles and bonding lengths vary from that of their crystalline counterparts thus resulting in the lack of long range atomic order. This produces the general irregular appearance of amorphous atomic structure a type of disorder termed as translational disorder.

The structure of amorphous solids can also be described by the models proposed by Mott and Davis, Cohen *et al* and Marshall and Owen.

These models shown in figure 3.3 provide a clear picture of the density distribution of states (DOS) in the energy gap of amorphous semiconductors.

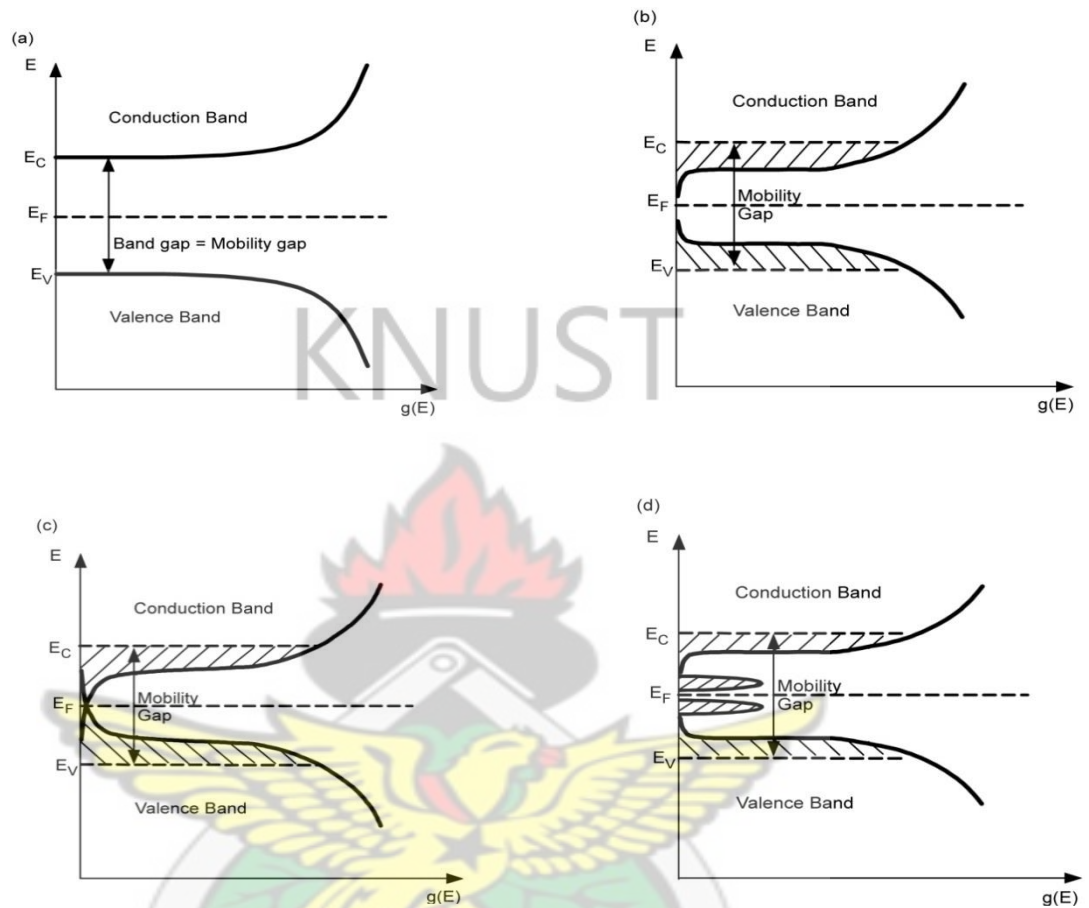


**Figure 3.3: (a) DOS of a crystalline semiconductor; (b) DOS models proposed by Mott, (c) DOS models proposed by Cohen, Fritzsche and Ovshinski, and (d) DOS models proposed by Marshall and Owen.**

These models illustrate the absence of DOS within the energy gap in crystalline semiconductors (c-semiconductors) whereas there exists a non-zero DOS within the mobility gap in amorphous semiconductors (a-semiconductors). It is now well established that these distinct features of the DOS of a-semiconductors arise due to the presence of tail states and gap states, which are localized states, and which do not exist in crystalline semiconductors (Mott and Davis, 1979; Cody, 1984). It is also well established that the origin of tail states is due to the absence of long range order

in a-semiconductors, and the presence of weak bonds such as dangling bonds. Unlike the extended states found in the two principal bands, electrons in the localized states are not free to travel anywhere in the material and thus have zero mobility thus they are confined within the localized states (trap states).

### 3.2. BASIC PRINCIPLES OF CHEMICAL BATH DEPOSITION (CBD)

The CBD technique is a convenient and non-sophisticated method for deposition of thin films. This method uses a controlled chemical reaction to deposit a thin film on a substrate. In a typical experiment, the substrates are immersed in a solution containing the chalcogenide source, metal ion, and complexing agent (Kassim *et al.*, 2009).

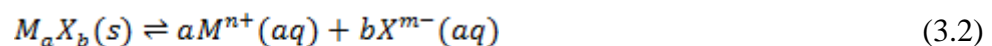
The basic principle behind the CBD process is based on the solubility product of the compounds. At equilibrium, the concentration of ions in the solution is defined by the solubility product (SP) equation (equation 3.1).

$$K_{sp} = [M^{n+}]^a [X^{m-}]^b \quad (3.1)$$

Where  $K_{sp}$  is the solubility constant and  $[M^{n+}]^a [X^{m-}]^b$  is the ionic product (IP).

The film formation occurs when the ionic product (IP) of the metal and chalcogenide ions exceed the solubility constant ( $K_{sp}$ ) of the corresponding chalcogenide ( $IP > K_{sp}$ ).

$aM^{n+}$  ions and  $bX^{m-}$  ions are formed from the solid as in equation 3.2.



The more soluble the salt, the greater the ionic product and the greater is  $K_{sp}$ . However,  $K_{sp}$  also depends on the number of ions involved. The concentration of metal ion in solution can be controlled by controlling the concentration of the complexing agent (Chopra *et al.*, 1982).

The main factors that govern CBD as well as control the rate of generation of metal ion and non-metal ion precursors are: Nature of reactants/precursor concentration, pH, deposition temperature, deposition time, nature of substrates and the complexing agent (Lakshmi, 2001).

**3.2.1. Nature of reactants/precursor concentration:** The nature of the reactants, influence the deposition process of metal chalcogenide generation. Estrada *et al.* (1994), Grozdanov (1994) and Garcia *et al.* (1999) reported that the preparation of copper selenide had a final phase of  $Cu_2Se$  when sodium selenosulfate was used as the selenium source as compared to the use of dimethylselenourea resulting in a  $CuSe$  phase. Also at high concentration, there is rapid precipitation of the metal ions, leading to a decrease in film thickness on the substrate.

**3.2.2. pH:** When the pH value of the reaction bath increases, the metal complex usually becomes more stable, reducing the availability of free metal ions. This will decrease the reaction rate resulting in higher thickness.

**3.2.3. Deposition time:** The growth of good quality semiconductor thin films proceeds to slow rate. This technique of CBD is ideally suited for producing uniform films with thickness in the 0.05- 0.3 $\mu m$  range in most cases (Lakshmi, 2001)

**3.2.4. Nature of substrates:** This factor plays an important role in the reaction mechanism and the adhesion of the deposited film. Hence, cleaning the substrate surface forms the first important step in the thin film deposition procedure.

**3.2.5. Complexing agent:** Nature of complexing agent may influence the final products. The metal ion concentration decreases with increasing concentrations in a general reaction. The rate of reaction and hence precipitation are reduced leading to a larger thickness of the film (Lakshmi, 2001).

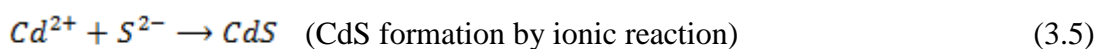
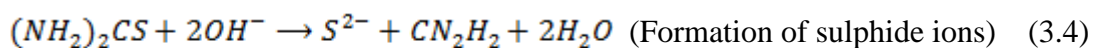
### 3.3. BASIC MECHANISM OF CBD

The mechanisms of the CBD processes can be divided into two different processes: formation of the required compound by ionic reactions involving free anions, and decomposition of metal complexes. Two main fundamental growth mechanisms have been identified (Froment et al., 1997; Gorer and Hodes, 1994):

- ❖ Ion by ion growth
- ❖ Cluster by cluster growth

Ion by ion growth is defined as the formation of chalcogenide nuclei on the surface of a substrate followed by subsequent growth on those nuclei (Froment *et al.*, 1997).

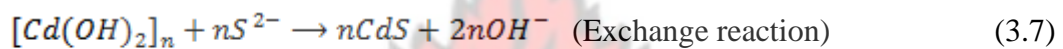
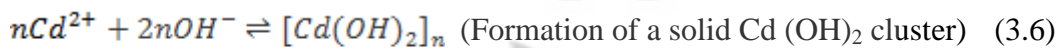
The basis of this mechanism, illustrated for CdS, in an alkaline medium is given by:



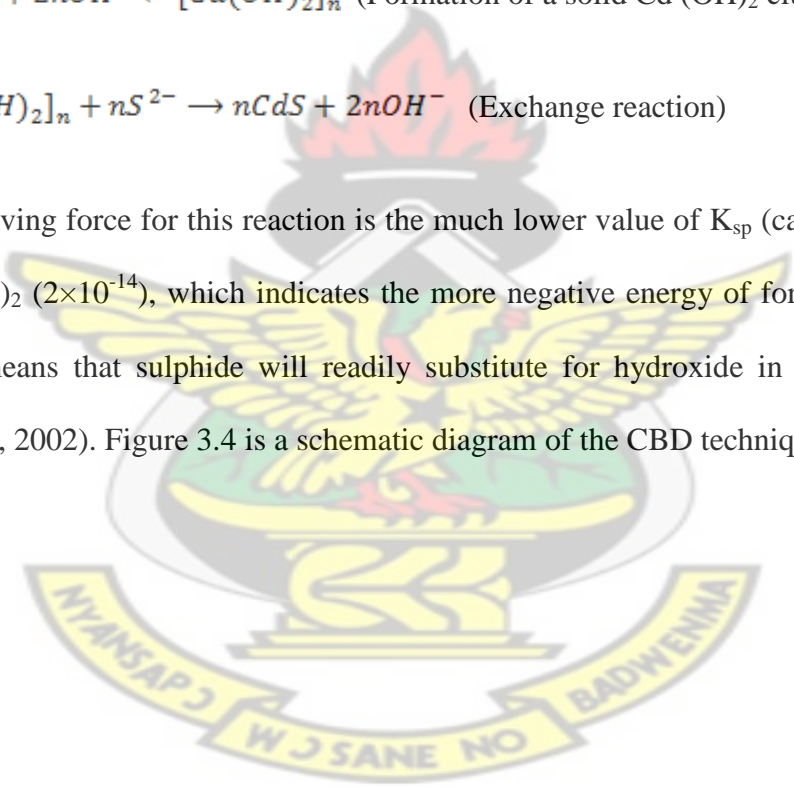
If the ion product,  $[Cd^{2+}][S^{2-}]$ , exceeds the solubility product,  $K_{sp}$ , of CdS (ca.  $10^{-28}$ ), then CdS can form as a solid phase, else no solid phase will form (this may not be

true under certain conditions). The mechanism involves the formation of  $S^{2-}$  ions and control of  $Cd^{2+}$  concentration (Hodes, 2002).

In the case of cluster by cluster growth, the initial step in the deposition is adhesion of the metal hydroxide to the substrate. This hydroxide is then converted into, e.g., CdS, forming a primary deposit of CdS clusters. More Cd (OH)<sub>2</sub> and, as the reaction proceeds, CdS and partially converted hydroxide diffuses/converts to the substrate, where it may stick, either to uncovered substrate (in the early stages of deposition) or to already deposited material. (Hodes, 2002)



The driving force for this reaction is the much lower value of  $K_{sp}$  (ca.  $10^{-28}$ ) than for Cd(OH)<sub>2</sub> ( $2 \times 10^{-14}$ ), which indicates the more negative energy of formation of CdS. This means that sulphide will readily substitute for hydroxide in the case of Cd (Hodes, 2002). Figure 3.4 is a schematic diagram of the CBD technique.



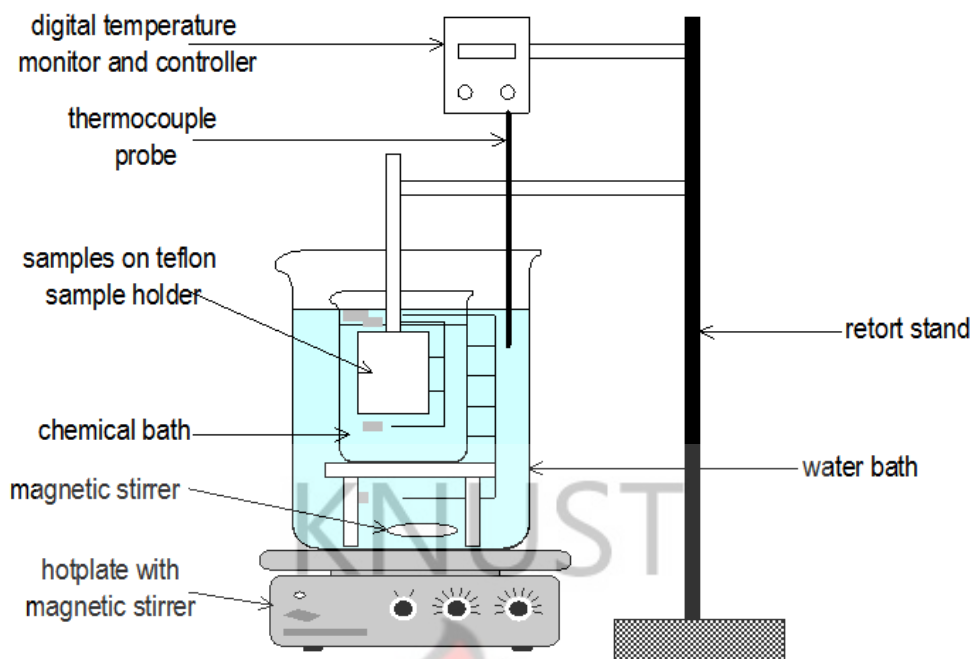


**Figure 3.4: Schematic diagram of Chemical Bath Deposition Technique**  
(Musembi et al., 2013)

### 3.4. THEORY OF THE CHARACTERIZATION TECHNIQUES.

Characterization (as applied in material science) refers to the use of external techniques to probe into the internal structure and properties of a material (en.wikipedia.org / wiki / characterization\_ (material\_science)). The purpose of characterization is to understand the microstructure characteristics which are responsible for the observed physical properties. Thin films are very sensitive to the deposition history and any change in the deposition conditions affects the microstructure characteristics which in turn also affects the observed physical properties.

Many techniques have been used to characterize thin films. Three common techniques used are transmission electron microscopy together with electron diffraction, powder X-ray diffraction (XRD), and optical absorption (or transmission) spectroscopy. In this thesis XRD and Optical absorption Spectroscopy were used to characterize the films and the precipitates.

### 3.4.1. OPTICAL ABSORPTION

The most direct and perhaps the simplest method for probing the band structure of semiconductors is to measure the absorption spectrum. In the absorption process a photon of known energy excites an electron from a lower to a higher energy level. In a semiconductor there exist allowed energy bands. Thus, there will be a range of photon energies that can be absorbed. By inserting a slab of semiconductor material at the output of a monochromator and studying the changes in the transmitted radiation, one can discover all possible transitions an electron can make and learn much about the distribution of states.

There are a number of possible transitions namely: band-to-band, excitons, between sub bands, between impurities and bands, transitions by free carriers within a band, and also resonances due to vibrational states of the lattice and of the impurities as shown in figure 3.5

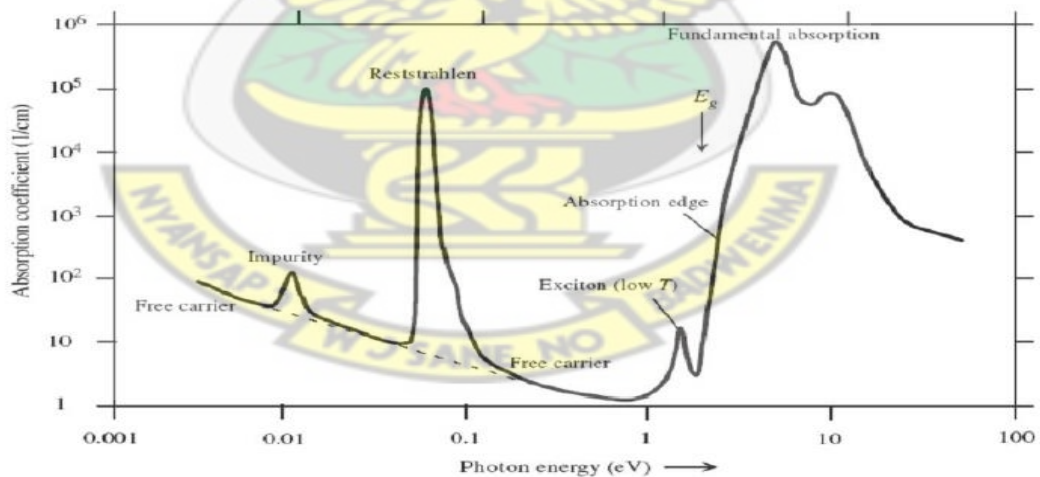


**Figure 3.5: Absorption coefficient plotted as a function of the photon energy in a typical semiconductor to illustrate the various possible absorption processes (Singh, 2006).**

Fundamental absorption refers to band-to-band transitions, i.e., the excitation of electrons from the valence band to the conduction band. The fundamental absorption

which manifests itself by a rapid rise in absorption can be used to determine the energy gap of the semiconductor. However, because the transitions are subject to certain selection rules (i.e. there are some restrictions based on the E-K diagrams), the estimation of the energy gap from the “absorption edge” is not a straightforward process. Absorption at the band edge depends on whether the material is a direct or indirect semiconductor. For a photon to be absorbed, and by conservation of energy, the energy of the system must be the same before and after the absorption event. Before the collision, of the electron and the photon, their combined energy is  $E_{\text{electron}} + E_{\text{photon}} = E_o + h\nu$ , where  $E_o$  is the initial electron energy. In the event that there is a collision between the photon and an electron, the photon transfers its energy to the electron causing the annihilation of the photon. By conservation of energy, now the electron has energy  $E_1 = E_o + h\nu$ , where  $E_1 > E_o$ .

Aside from the conservation of energy, there is also the law of conservation of wave vector  $K$  (analogous to conservation of momentum in classical mechanics). Photons of interest in semiconductor electronics have wave vectors that are small and in most cases can be considered to be essentially zero. Therefore, when the electron makes an energy transition, it must do so at virtually constant  $K$ , which is to say it must make a vertical transition on the E-K diagrams as shown in figure 3.6.

Semiconductors for which the minimum of the conduction band occurs at the same wave vector,  $K$ , as the maximum of the valence band are referred to as direct band gap semiconductors

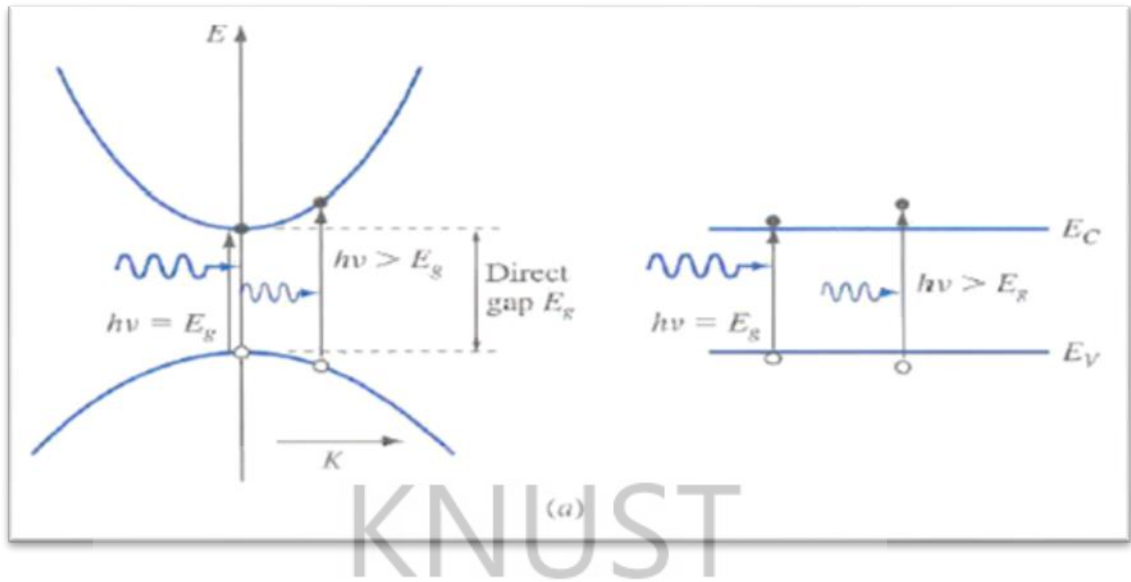


**Figure 3.6: Diagram of a direct band gap semiconductor**

In direct band gap materials, when an electron acquires enough energy, it can make a transition from the edge of the valence band to the edge of the conduction band, when the maximum of the valence band is at the same wave vector,  $K$ , as the minimum of the conduction band. Direct band gap semiconductors have a stronger absorption of light as a result of a larger absorption coefficient. Direct band gap materials are generally efficient emitters and absorbers of optical energy because it is easy for electrons to move between the conduction and valence band without having to acquire or give off  $K$  (wave vector). They are also the appropriate semiconductors for fabrication of light emitting devices. Typical examples are CdSe, CuSe, CdS, CuS, GaAs, and ZnS.

An indirect gap material, on the other hand, is one like that shown in figure 3.7 where the minimum of the conduction band does not occur at the same wave vector,  $K$ , as the maximum of the valence band.

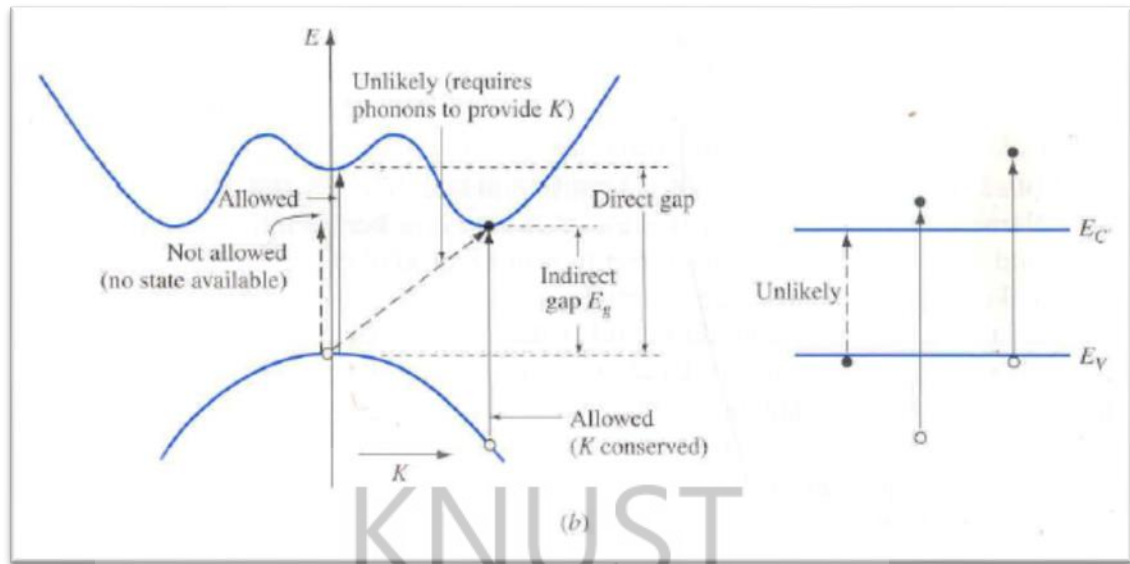


**Figure 3.7: Diagram of an indirect band gap semiconductor.**

In indirect band gap materials, an electron cannot go from one band to another simply by absorbing a photon of energy close to the band gap, because the photon cannot supply adequate wave vector. The electron needs to acquire both energy and wave vector to make the transition in indirect materials. At the band edges, there is the need for a three particle collision. This three-particle collision involves an electron, a photon and a phonon. Phonons have adequate wave vector ( $K$ ) but have little energy, while the opposite is true for photons. If a photon and a phonon collide with an electron at the same time, the electron acquires both enough energy and enough  $K$  to overcome the forbidden gap. Such a three-body collision is quite often unlikely. Examples of such materials are Si, Ge, and GaP.

#### **3.4.1.1. DETERMINATION OF THE OPTICAL BAND GAP**

Absorption is expressed in terms of a coefficient,  $\alpha (h\nu)$  which is defined as the relative rate of decrease in light intensity along its propagation path. The absorption coefficient,  $\alpha$ , is a property of a material which defines the amount of light absorbed

by it.

The absorption is governed by the Beer Lambert law:

$$I = I_0 \exp(-\alpha t) \quad (3.8)$$

where  $I_0$  is the incident radiation intensity,  $\alpha$  is the absorption coefficient,  $I$  is the transmitted light intensity and  $t$  is the thickness of the film.

The absorbance is given by the logarithmic ratio of the incident light to the transmitted light intensities. The spectrophotometer operates on this principle by measuring the ratio of incident to transmitted light intensity.

Mathematically,

$$A = \log\left(\frac{I_0}{I}\right) \quad (3.9)$$

where  $A$  =Absorbance,  $T$  or  $I$  =Transmitted light intensity,  $I_0$  =Incident light intensity.

The band gap can be determined from optical absorption measurements by using the Tauc relation which is expressed as:

$$\alpha h\nu = B(h\nu - E_g)^n \quad (3.10)$$

where  $\alpha$ , is the optical absorption coefficient,  $B$  is a transition probability constant that depends on the films material,  $h\nu$  is the energy of the incident photon,  $E_g$  is the optical band gap, and  $n$  is an index dependent on the type of electronic transition. In a direct transition  $n$  is equal to  $1/2$  and  $3/2$  for allowed and forbidden transitions

respectively. For indirect transition,  $n$  is equal to 2 for allowed transitions and 3 for forbidden transitions (Wood and Tauc, 1972; Davis, 1993).

From equation (3.10) for direct allowed transition and constant  $B$ , we obtained

$$\alpha hv = B(hv - E_g)^{\frac{1}{2}} \quad (3.11)$$

A plot of  $(\alpha hv)^2$  against  $hv$  is linear over a wide range of photon energies, indicating the direct type of transitions. The energy band gap is determined by extrapolating the linear portion of  $(\alpha hv)^2$  versus  $hv$  to the energy axis at  $(\alpha hv)^2 = 0$ . The intercepts of these plots on the energy axis gives the energy band gap (Tauc, 1974; Yacobi, 2004). An alternative method for determining the band gap is to use the Stern (1963) relation which is expressed mathematically as:

$$(Ahv) = [K(hv - E_g)]^{\frac{n}{2}} \quad (3.12)$$

where  $hv$  is the photon energy,  $A$  is the absorbance;  $K$  equals a constant while  $n$  carries the value of either 1 or 4. In a direct transition  $n$  is equal to 1 and 4 for allowed and forbidden transitions respectively. The band gap,  $E_g$ , could be obtained from a straight line plot of  $(Ahv)^{2/n}$  as a function of  $hv$ . Extrapolation of the line to intersect the horizontal axis at  $(Ahv)^{2/n} = 0$ , will give the energy band gap as shown in figure 3.8

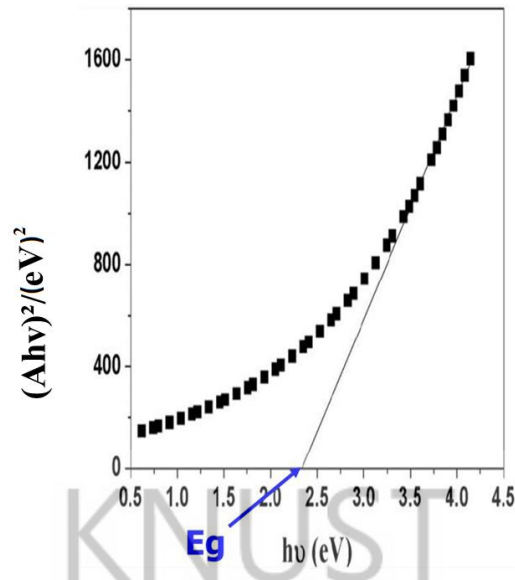


**Figure 3.8:** Shows a plot of  $(Ahv)^2$  against  $hv$  as proposed by Stern (1963)

### 3.4.2. X-RAY DIFFRACTION

X-rays are penetrating electromagnetic radiation with wavelength ranging from about 0.01 Å to 10 Å and are produced when high-speed electrons bombard a metal target (mostly tungsten). X-rays can be diffracted when passing through a crystal or by reflection from a crystal with a regular lattice of atoms that serve as fine diffraction gratings (Redmond, 2008).

#### 3.4.2.1 BRAGG FORMULATION OF X-RAY DIFFRACTION BY A CRYSTAL

In crystalline materials, for certain sharply defined wavelengths and incident directions, intense peaks of scattered radiation (known as Bragg peaks) are observed. Sir W.H. Bragg and his son Sir W.L. Bragg in 1913 developed a relationship to explain why the splitting faces of crystals appear to reflect X-ray beams at certain angles of incidence (theta,  $\theta$ ). This observation is an example of X-ray wave interference commonly known as X-ray diffraction (XRD), and is a direct evidence for the periodic atomic structure of crystals postulated for several centuries. The conditions that satisfy such Bragg peaks are:

- ❖ that the X rays should be specularly (mirror-like) reflected by atoms in any one plane
- ❖ that the reflected rays from successive planes should interfere constructively (Ashcroft and Mermin, 1976).

When a monochromatic beam of x-ray enters the crystal, some portion of it will be reflected by the first atomic plane, while the rest will continue through to the second layer where the process continues. By definition of *constructive interference*, the separately reflected waves will remain in phase if the difference in path length between the waves is equal to an integer multiple of their wavelength. Thus according to the Bragg condition, constructive interference occurs when

$$2d \sin \theta = n\lambda \dots\dots\dots 3.13, \text{ where:}$$

- $n$  is an integer.
- $\lambda$  is the wavelength of electrons (wave).
- $d$  is the spacing between the planes in the atomic lattice, and
- $\theta$  is the angle between the incident ray and the scattering planes.

The reflection condition in equation 3.13 is called the *Bragg condition*. Figure 3.9 illustrates constructive interference referred to as the Bragg's law of diffraction.

For normal incidence of the electron wave ( $\theta = 90^\circ$ ), the Bragg condition can be expressed as:

$$\lambda = \frac{2d}{n} \dots\dots\dots 3.14$$

The wave vector  $k$  can be expressed as  $k = 2\pi/\lambda$ , and from equation 3.14,

$$k = \frac{\pi n}{d} \dots\dots\dots 3.15, \text{ for } n = \pm 1, \pm 2, \pm 3 \dots\dots$$

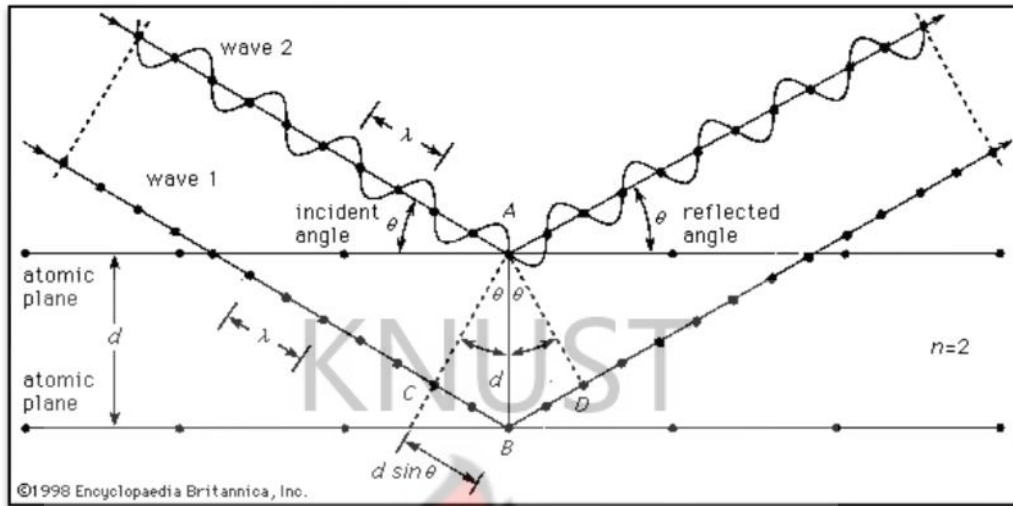


**Figure 3.9: Illustration of Bragg's law of Diffraction**

The scattering of X-rays from atoms produces a diffraction pattern, which contains information about the atomic arrangement within the crystal ([www.prism.mit.edu](http://www.prism.mit.edu)). This technique is termed as the X-Ray diffraction technique. This technique is the most suitable, non-destructive and most precise method for crystal structure analysis and atomic spacing. It is simple because no elaborate sample preparation is required (Chopra and Das, 1983; Schroder, 1998). A schematic illustration of an x-ray diffraction is shown in figure 3.10.

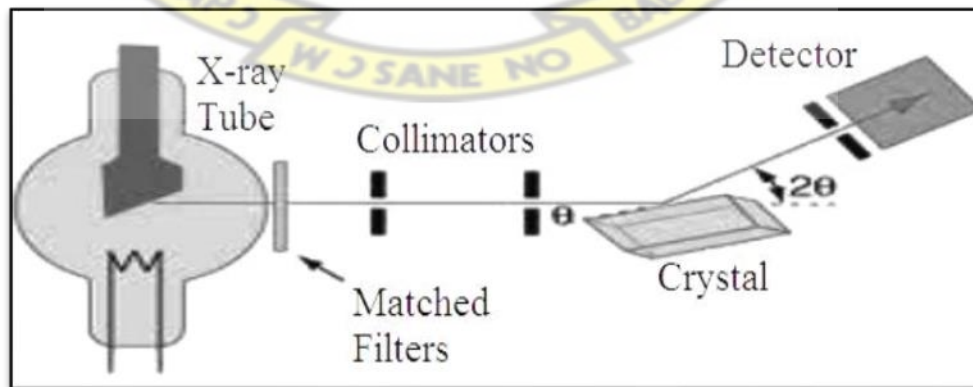


**Figure 3.10: Schematic Diagram for X-ray Diffraction (Wikipedia/braggs law).**

### 3.4.2.2 POWDER X-RAY DIFFRACTION

Powder XRD (X-ray Diffraction) is the most widely used x-ray diffraction technique for characterizing materials. The term 'powder' denotes that the crystalline domains are randomly oriented in the sample. Therefore, when the 2-D diffraction pattern is recorded, it shows concentric rings of scattered peaks corresponding to the various d-spacing in the crystal lattice. Powder diffraction data can be collected using transmission or reflection geometry, as shown in figure 3.11 since particles in the powder sample are randomly oriented.

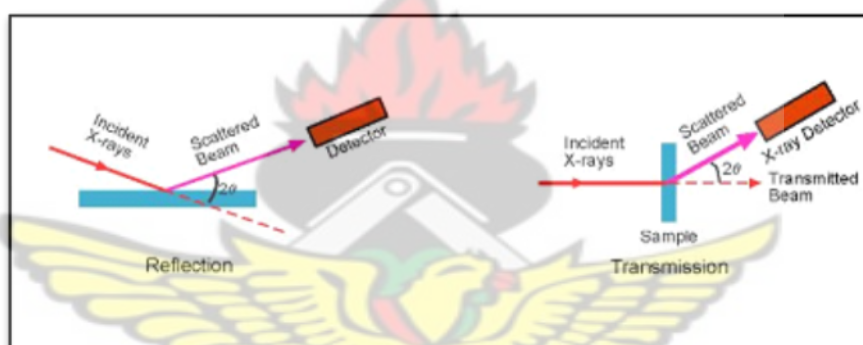


**Figure 3.11. Illustration of the Reflection and Transmission geometry**

In the powder X-ray diffractometer, x-rays are generated within a sealed tube which is kept in vacuum. A high voltage, typically 15-60 kilovolts and a current which heats the filament is applied within the tube; a higher current emits a greater number of electrons from the filament. This high voltage accelerates the electrons, which then hits a target, usually copper. When these electrons hit the target, X-rays are produced. The wavelength of these X-rays is characteristic of that target. These X-rays are collimated and directed onto the material to be analyzed. Powdered samples are made up of randomly oriented crystallites. For every set of planes, there will be a small percentage of crystallites that are properly oriented to diffract. The diffracted radiation is detected by the counter tube and the intensities recorded on a computer.

The x-ray diffraction data is compared to a standard database to confirm the material. The crystallite size of the sample is estimated using the Scherrer (1918) formula as follows

$$D = \frac{0.9\lambda}{\beta \cos\theta} \quad 3.15$$

where  $D$  is the crystallite size,  $\lambda$  is wavelength of X-ray used,

$\beta = (2\theta \text{ High}) - (2\theta \text{ Low})$  is full width at half maxima of the peak (FWHM) in

radians,  $\theta$  is Bragg's angle. The X- ray diffraction data can also be used to determine

the dimension of the unit cell. A schematic illustration of the rotating crystal method of x-ray diffraction is shown in figure 3.12

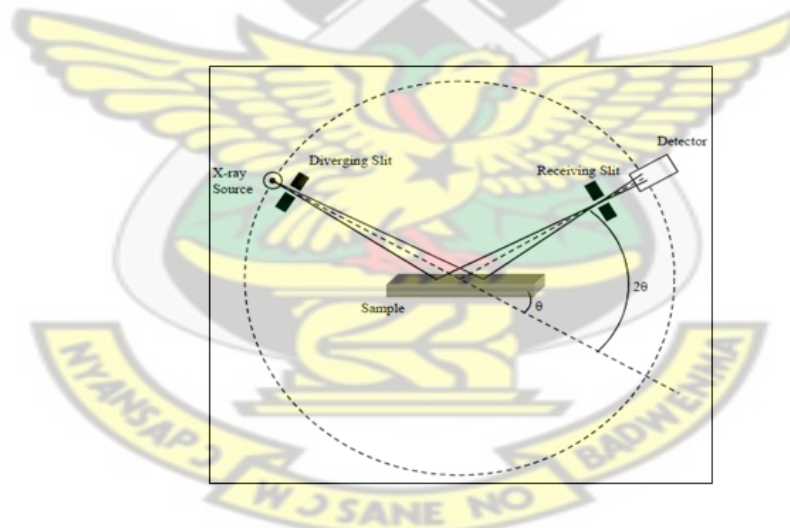


**Figure 3.12: Schematic diagram of the rotating crystal method of X-ray diffraction**

## CHAPTER FOUR

### 4.0. METHODOLOGY

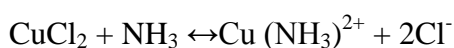
#### 4.1 SUBSTRATE PREPARATION.

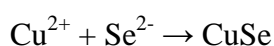
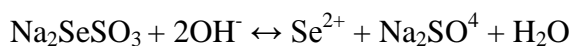
Substrate cleaning is a very important process in thin film preparation. The purpose of substrate cleaning is to enhance proper film adhesion onto the substrate and to allow for smooth and uniform deposition. The substrates are also cleaned to remove all unwanted particulate matter on it before deposition. The silica glass slides were thoroughly washed by soaking them overnight in nitric acid and washed in distilled water, placed in ethanol for 30 minutes and washed with distilled water and allowed to dry before usage. The ethanol was to de-grease the slides.

#### 4.2 PREPARATION OF COPPER SELENIDE THIN FILMS

Starting reagents containing appropriate amounts of  $\text{CuCl}_2$  solution,  $\text{NH}_3$  and  $\text{Na}_2\text{SeSO}_3$  (Sodium selenosulphate) (all of analytical reagent grade) were mixed in a 100 ml beaker and the pH set. The solution was then placed in a water bath kept at the optimum temperature for deposition. Two chemically cleaned glass slides were fixed in a holder and placed vertically in the beaker. The mixture was then left to allow for  $\text{Cu}_{2-x}\text{Se}$  film deposition. After some time, the substrates were taken out and washed with distilled water and any adherent particulate matter removed and allowed to dry under ambient conditions. The above process was repeated for four other glass slides.

The equation for the process is given as:

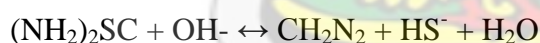




### 4.3 PREPARATION OF COPPER SULPHIDE THIN FILMS

A mixture containing appropriate amounts of  $\text{CuCl}_2$  solution,  $\text{NH}_3$  and  $\text{CH}_4\text{N}_2\text{S}$  (Thiourea) (all of analytical reagent grade) was prepared in a 100 ml beaker and placed on a magnetic hotplate stirrer. The solution was then placed in a water bath kept at an appropriate temperature and continuously stirred by a magnetic stirrer. Two dried glass slide were fixed in a cork and placed vertically in the beaker. The mixture was then left for some time to allow for  $\text{Cu}_x\text{S}$  film deposition. The substrates were taken out and washed with distilled water to remove any adherent particulate matter and allowed to dry under ambient conditions. The above process was repeated for four other glass slides.

The equation for the reaction process is:



The concentration of the reagents, the pH and the deposition time used for the deposition of  $\text{CuSe}$  and  $\text{Cu}_x\text{S}$  samples are different from those used by other authors.

Figure 4.1 describes the experimental setup of the chemical bath deposition technique.

**Figure 4.1. Experimental set-up of a CBD**

#### **4.4 METHODOLOGY FOR OPTICAL ABSORPTION MEASUREMENTS**

The absorbance (A) spectra of the deposited thin films were obtained, using a UV mini Shimadzu UV-VIS spectrophotometer (model: UV mini-1240) within a wavelength range of 300 nm to 1100 nm at room temperature. The as-deposited films along with a plane slide used as a reference slide were mounted on a rotating holder at the reference and sample compartments, respectively, and scanned to obtain the absorbance spectra. The absorbance measurement was also carried out after each annealing process.

#### **4.5 METHODOLOGY FOR X-RAY DIFFRACTION**

The crystallographic structure of  $\text{Cu}_x\text{S}$  and  $\text{Cu}_{2-x}\text{Se}$  samples were analyzed with a PANalytical Empyrean series 2 powder XRD with a Cu  $k_\alpha$  radiation (1.54060 Å) source over the diffraction angle  $2\theta$  between  $20^\circ$  and  $70^\circ$  and operating with an accelerating voltage and current of 45 kV and 40 mA respectively. The samples were finely ground and homogenized and pressed into a sample disc and placed in the sample holder of the X-ray diffractometer. The diffractometer uses the Bragg-Brentano geometry. The samples were run through a flat stage and a spinner stage between 15 to 40 minutes with a zero background to eliminate or minimize the amount of noise present in the data. The zero background produces X-ray peaks from only the sample. The diffracted radiation was detected by the counter tube and the intensities were recorded on a computer system. The X-ray data was analyzed using the High score Plus software which has an incorporated database as a point of reference comparison. This process was repeated for the annealed samples.

## CHAPTER FIVE

### 5.0 RESULTS AND DISCUSSION

#### 5.1 COPPER SULPHIDE ( $\text{Cu}_x\text{S}$ )

##### 5.1.1 OPTICAL ABSORPTION

The optical absorption spectra of the various deposited films were obtained and analyzed at room temperature over the wavelength range from 300 nm to 1100 using a Shimadzu UV-VIS Spectrophotometer (UV mini 1240).

**Figure 5.1: A plot of Absorbance against Wavelength for as-deposited and annealed  $\text{Cu}_x\text{S}$  thin film at different temperatures.**

Figure 5.1 shows the absorption spectra of the as-deposited and annealed  $\text{Cu}_x\text{S}$  thin films. The films were annealed for an hour at temperatures of 573 K and 673 K and showed a decrease in absorbance after annealing. From the graph, the annealed films had slightly lower absorbance values than the as-deposited film and there was no significant decrease in the absorbance after annealing at 673 K as compared to the films annealed at 573 K. A possible explanation of the decrease in absorbance after annealing may be due to minimizing structural imperfections in the chemically prepared thin films resulting in density of fewer defect states within the band gap available for electron transitions, hence the lower absorbance readings. A similar decrease in absorbance after annealing was reported by Offiah et al. (2012) who reported that the as-deposited  $\text{Cu}_x\text{S}$  thin films showed 90 % absorbance while films annealed at 473 K showed 50 % and films annealed at higher temperatures (573 K and 673 K) showed very low absorbance values (< 20 %). It is obvious from the optical spectra that the fundamental absorption edges of samples shifted towards

shorter wavelengths (blue shift) after annealing. Similar observations have been reported by Hodes (2002). According to Kale and Lokhande (2000), the blue shift may be due to the fact that a smaller particle size will result in an absorption edge at smaller wavelength. The as-deposited films were blue-black and changed to black after annealing.

#### 5.1.1.1 DETERMINATION OF OPTICAL BAND GAP

Study of materials by means of optical absorption provides a simple method for explaining some features concerning the band structure of materials (Ubale *et al.*, 2007).

From the absorption spectra, the optical band gaps of the films were estimated using the Stern (1963) relation for near edge absorption given as:

$$A = \frac{[K(h\nu - E_g)]^{n/2}}{h\nu} \quad 5.1$$

where  $\nu$  is the frequency,  $h$  is the Planck's constant,  $K$  is a constant while  $n$  carries the value of either 1 or 4 which is for direct and indirect transitions respectively. The band gap was evaluated by extrapolating the linear portion of  $(A h\nu)^2$  versus  $h\nu$  to the energy axis at  $(A h\nu)^2 = 0$ .  $\text{Cu}_x\text{S}$  is known to be a direct band gap semiconductor, thus  $n$  takes the value of 1. The linear nature of the plots indicates the existence of direct transitions.

Figures 5.2, 5.3 and 5.4 show the band gap of as-deposited and annealed  $\text{Cu}_x\text{S}$  thin films respectively. The films were annealed at 573 K and 673 K.

**Figure 5.2: A plot of  $(A h\nu)^2$  vs  $h\nu$  for as-deposited  $\text{Cu}_x\text{S}$  thin film**

**Figure 5.3: A plot of  $(Ah\nu)^2$  vs  $h\nu$  for  $Cu_xS$  thin film annealed at 573 K**

**Figure 5.4: A plot of  $(Ah\nu)^2$  vs  $h\nu$  for  $Cu_xS$  thin film annealed at 673 K**

The optical band gap values were determined to be 1.62 eV for as- deposited and 2.22 eV after annealing at 573 K and 673 K. These compare favourably well with values reported in literature (Kırmızıgül *et al.*, 2013; Ilenikhena, 2008; Offiah, 2012; Santos *et al.*, 2012; Singh *et al.*, 2013). The  $Cu_xS$  thin films exhibited an increase in band gap after annealing. Similar observations have been reported by Asogwa *et al.* (2009). From the results, it was obvious that even after annealing at 673 K, there was no change in the band gap compared to the sample annealed at 573 K.

### 5.1.2 X-RAY DIFFRACTION

Figure 5.5 shows the powder x-ray diffraction pattern of copper sulphide. The horizontal axis of the graph is the  $2\theta$  angles and the vertical axis is the intensity/X-ray count rate which is a function of the crystal structure and the orientation of the crystallites.

**Figure 5.5: XRD pattern of copper sulphide as-deposited sample**

Figure 5.5 describes the XRD spectrum for as- deposited copper sulphide samples. The as-deposited powder showed several peaks confirming the polycrystalline nature of the sample. The sample contained a mixture of copper sulphide and copper sulphate phases. Predominant phases for the as-deposited sample were covellite and brochantite. The covellite phase had the highest score as seen in table 5.1. Most of the intense peaks were matched to the covellite phase. The peak positions ( $2\theta$  values) at  $31.75^\circ$ ,  $32.14^\circ$ ,  $47.83^\circ$ ,  $29.21^\circ$ ,  $59.17^\circ$ ,  $38.72^\circ$  correspond to reflections from the (103), (006), (110), (102), (116), (105) planes of the hexagonal covellite phase.

Similar observations of the presence of several phases in CBD copper sulphide were reported by Pop *et al.* (2011). The average grain size was calculated using the Scherrer (1918) formula in equation 3.15

$$D = \frac{0.9\lambda}{\beta \cos\theta} \quad 3.15$$

and found to be: 6.49 nm.

**Table 5.1. Summary of the structural properties and score of as-deposited copper sulphide samples.**

| <u>Visible Ref.Code</u>                                       | <u>Score</u> | <u>Compound Name</u> | <u>Cryst. Syst.</u> |
|---|--------------|----------------------|---------------------|
| <u>Chem. Formula</u>  |              |                      |                     |
| 96-101-0956 CuS   | 33           | Covellite            | Hexagonal           |
| 96-900-5584 Cu <sub>4</sub> SO <sub>4</sub> (OH) <sub>6</sub> | 23           | Brochantite          | Monoclinic          |

**Figure 5.6: XRD pattern of Cu<sub>x</sub>S powder annealed at 673 K**

Figure 5.6 is the XRD pattern of copper sulphide sample annealed at 673 K. The sample contained a mixture of copper sulphate pentahydrate and Antlerite phases as shown in table 5.2. Copper sulphate pentahydrate had the highest score and was the predominant phase. The peak positions ( $2\theta$  values) at  $22.278^\circ$ ,  $23.929^\circ$ ,  $26.916^\circ$ ,  $31.594^\circ$ , and  $32.456^\circ$  corresponded to reflections from the (102), ( $\bar{1}02$ ), ( $1\bar{1}1$ ), ( $122$ ) and ( $0\bar{1}3$ ) planes of the anorthic copper sulphate pentahydrate phase (COD 96-101-0528). The average grain size was calculated using the Scherrer (1918) formula

$$D = \frac{0.9\lambda}{\beta \cos\theta}$$

3.15

and found to be: 40.0 nm. The average grain size of the copper sulphide sample increased from 6.49 nm to 40.0 nm after annealing. The increase in the grain size agrees with report by Offiah et al. (2012), who reported an increase in the average grain size after annealing at 673 K. According to Hodes (2002), thin films annealed at temperatures above 573 K usually exhibited a large degree of crystal growth.

**Table 5.2. Summary of the structural properties and score of annealed copper sulfide samples.**

| <u>Visible Ref.Code</u>  | <u>Score</u> | <u>Compound Name</u>         | <u>Cryst. Syst.</u> |
|--|--------------|------------------------------|---------------------|
| <u>Chem. Formula</u>   |              |                              |                     |
| 96-101-0528<br>H <sub>10</sub> Cu <sub>1</sub> O <sub>9</sub> S <sub>1</sub> | 44           | Copper sulphate pentahydrate | Anorthic            |
| 96-901-3963<br>Cu <sub>3</sub> (SO <sub>4</sub> )(OH) <sub>4</sub>           | 41           | Antlerite                    | Orthorhombic        |

## 5.2 COPPER SELENIDE

### 5.2.1 OPTICAL ABSORPTION

The optical absorption spectra of the various deposited films were obtained and analyzed at room temperature over wavelength range from 300 nm to 1100 nm using a Shimadzu UV-VIS Spectrophotometer (UV mini 1240).

Figure 5.7 shows the absorption spectra of the as-deposited and annealed copper selenide thin films. The films were annealed for an hour at temperatures of 473 K, 573 K and 673 K.

**Figure 5.7: A plot of Absorbance against Wavelength for as-deposited and annealed Cu<sub>2-x</sub>Se thin film at different temperatures.**

The films showed an increase in absorbance as annealing temperature increased. The most significant change in absorbance value was evident after annealing at 673 K. The increase in absorbance with annealing suggests an increase in grain size. Annealing therefore produced a good absorber. This agrees with report by Usoh and Okujagu (2014) on the absorption of CuSe thin films. The fundamental absorption edges of samples also shifted towards longer wavelengths (red shift) as annealing temperatures increased. These red shifts may be attributed to an increase in particle size which was confirmed by the XRD analysis. Juska *et al.* (2010) attributed a similar red shift in copper selenide nanowires deposited by alternating current electro-deposition to a common feature of nanostructures containing double valence copper (eg. CuSe, CuFeS<sub>2</sub>). Middle gap states are formed in these compositions. We may also attribute an improvement in the crystallinity of the sample to the shift. The as-deposited films were blue-black and changed to bluish green after annealing. The colour change is in agreement with reported observation by Lakshmi (2001), indicating a typical Cu<sub>3</sub>Se<sub>2</sub> phase.

### 5.2.1.1 DETERMINATION OF OPTICAL BAND GAP

The optical band gaps of the films were determined using equation 5.1

$$A = \frac{[K(h\nu - E_g)]^{n/2}}{h\nu} \quad 5.1$$

Figure 5.8 shows the band gap of as-deposited  $\text{Cu}_{2-x}\text{Se}$  thin film and Figures 5.9, 5.10 and 5.11 shows the band gap of annealed  $\text{Cu}_{2-x}\text{Se}$  thin films. The band gap was evaluated by extrapolating the linear portion of  $(Ah\nu)^2$  versus  $h\nu$  to the energy axis at  $(Ah\nu)^2 = 0$ .

**Figure 5.8: A plot of  $(Ah\nu)^2$  vs  $h\nu$  for as-deposited  $\text{Cu}_{2-x}\text{Se}$  thin film**

**Figure 5.9: A plot of  $(Ah\nu)^2$  vs  $h\nu$  for  $\text{CuSe}$  thin film annealed at 473 K.**

**Figure 5.10: A plot of  $(Ah\nu)^2$  vs  $h\nu$  for  $\text{CuSe}$  thin film annealed at 573 K**

**Figure 5.11: A plot of  $(Ah\nu)^2$  vs  $h\nu$  for  $\text{CuSe}$  thin film annealed at 673 K**

The optical band gap values were determined to be 1.2 and 1.4 eV for as-deposited and 0.9 to 2.2 eV after annealing respectively. These compare favourably well with values reported in literature (Al-Mamun *et al.*, 2005; Sorokin *et al.*, 1996; Okimura *et al.*, 1980; Khomane, 2012). The presence of two band gap values for as deposited samples may be attributed to the presence of more than one phase. This was confirmed in the X-ray diffraction analysis. The presence of two band gaps was also observed in the samples annealed at 473 K, indicating that annealing did not produce any change in the phases present. The  $\text{Cu}_{2-x}\text{Se}$  films showed a decrease in the band gap after annealing at 473 K and a rather great increase at higher annealing temperatures. The decrease in the band gap after annealing at 473 K is not quite clear and further investigations should be done. However, after annealing at 573 K and 673 K, only one phase was observed suggesting the presence of a single phase. According to Al-Mamun *et al.* (2005), the increase in band gap due to annealing may be understood by the improvement of crystallinity of the as-deposited film on

annealing as observed in the XRD analysis. They reported well defined peaks suggesting the improvement of crystallinity of the film due to annealing at high temperature. This increase is in agreement with reported observation by Rajesh *et al.* (2013) and the decrease also agrees with reported behavior by Bari *et al.* (2009). According to Hodes (2002), other studies on chemically deposited Cu-Se, showed that Cu-Se has a tendency to form relatively large crystals. This may be due, at least in part, to the high mobility of  $\text{Cu}^{2+}$  and the relatively low melting point of the Cu-Se compounds in general.

## 5.2.2 X-RAY DIFFRACTION

### Figure 5.12 XRD pattern of as-deposited Copper selenide

Figure 5.12 shows the XRD pattern of copper selenide obtained through the chemical bath deposition method. The presence of several peaks in the XRD traces confirmed the polycrystalline nature of the sample. From the as-deposited XRD pattern, the peaks indicated the formation of a heterogeneous phase of  $\text{Cu}_3\text{Se}_2$ , CuSe and  $\text{Cu}_{2-x}\text{Se}$ . The results matched well with the standard COD values for  $\text{Cu}_3\text{Se}_2$ , for CuSe and for  $\text{Cu}_{2-x}\text{Se}$ .

From the XRD results, the  $\text{Cu}_3\text{Se}_2$  (Umangite) phase had the highest score as seen in table 5.3 defining the dominant peaks. The peak positions ( $2\theta$  values) at  $24.96^\circ$ ,  $27.79^\circ$ ,  $27.78^\circ$ ,  $31.03^\circ$ ,  $44.63^\circ$ ,  $45.19^\circ$ ,  $49.68^\circ$  and  $51.24^\circ$  corresponding to reflections from the (101), (102) (200), (006), (220), (310), (221), (311), (202) planes of the tetragonal Umangite phase (File no. 96-900-9857). A similar structure was reported by Soon (2011) where the preferred orientation was along the (006) plane corresponding to peak position ( $2\theta$  value) at  $31^\circ$  of the hexagonal copper selenide thin film. He also reported a peak position ( $2\theta$  value) at  $25^\circ$  corresponding

to reflections from the (101) plane. The average grain size was calculated using the Scherrer (1918) formula in equation 3.15 and found to be 27.3 nm.

$$D = \frac{0.9\lambda}{\beta \cos\theta} \quad 3.15$$

**Table 5.3: Summary of the structural properties and score of as-deposited copper selenide sample.**

| <u>Visible Ref.Code</u>                        | <u>Score</u> | <u>Compound Name</u> | <u>Displ.[°2θ]</u> | <u>Cryst. Syst.</u> |
|--|--------------|----------------------|--------------------|---------------------|
| <u>Chem. Formula</u>                           |              |                      |                    |                     |
| 96-900-9857<br>Cu <sub>3</sub> Se <sub>2</sub> | 63           | Umangite             | 0.000              | Tetragonal          |
| 96-900-0064<br>CuSe                            | 40           | Klockmannite         | 0.000              | Hexagonal           |
| 96-900-8067<br>Cu <sub>2-x</sub> Se.           | 41           | Berzelianite         | 0.000              | Cubic               |

**Figure 5.13 XRD pattern of Copper selenide annealed at 673 K**

The XRD profile presented in figure 5.13 shows the pattern of copper selenide annealed at 673 K. The CuSe<sub>2</sub> (Krutaite) phase was most dominant with the highest score as seen in table 5.4. Three peak positions (2θ values) at 33.29<sup>0</sup>, 41.72<sup>0</sup> and 58.43<sup>0</sup> corresponded to reflections from the (111), (121), and (022) planes of the orthorhombic krutaite phase. The preferred orientation was along the (111) plane.

After annealing, the average grain size was calculated using the Sherrer (1918) formula and found to be 41.6 nm indicating an increase in grain size. The increase compares well with reported observation in literature (Hodes, 2002), that chemically deposited Cu-Se, has a tendency to form relatively large crystals.

**Table 5.4: Summary of structural properties and score of annealed copper selenide samples**

| <u>Visible Ref.Code</u>       | <u>Score</u> | <u>Compound Name</u> | <u>Cryst. Syst.</u> |
|-------------------------------|--------------|----------------------|---------------------|
| <u>Chem. Formula</u>          |              |                      |                     |
| 96-410-5299 CuSe <sub>2</sub> | 13           | Krutaite             | Orthorhombic        |

KNUST



## CHAPTER SIX

### 6.0 CONCLUSIONS AND RECOMMENDATION

#### 6.1. CONCLUSIONS

Thin films of copper sulphide and copper selenide were successfully deposited using the chemical bath deposition technique in an alkaline medium. The investigations of the optical band gap and structure were successfully carried out using optical absorption spectroscopy and powder x-ray diffraction analysis.

The results of the optical measurements showed that thin films of copper sulphide had a band gap of 1.6 eV for the as-deposited samples and 2.2 eV after annealing. The structural analysis showed the presence of several phases in the as-deposited sample with the covellite phase being dominant. After annealing the dominant phase was copper sulphate pentahydrate.

The as-deposited copper selenide films possessed two band gaps of 1.2 and 1.4 eV which may suggest the presence of two phases. After annealing at 573 K and 673 K, the band gap was 2.2 eV at both temperatures. The structural analysis of the copper selenide samples showed the presence of several phases but the dominant phase was umangite. After annealing, the dominant phase was the krutaite. There was an increase in the average grain size in the copper sulphide and copper selenide samples after annealing suggesting a further crystal growth at these temperatures. The energy band gap of copper sulphide and copper selenide films were found to increase after annealing. The results obtained in this work are in agreement with values reported in literature. However, the concentration of the reactants, pH and deposition time are different from those reported in literature. This work therefore provides a unique set

of deposition parameters suitable for the growth of  $\text{Cu}_x\text{S}$  and  $\text{CuSe}$  thin films. In addition, the similarities in the deposition conditions for both compounds open up the possibility of depositing the ternary films of  $\text{CuSSe}$ .

## 6.2 RECOMMENDATIONS

Even though the deposition carried out was successful, a few questions still remain unanswered and further investigation should be carried out in the following areas:

- ❖ An investigation into the morphology of the thin film by carrying out Scanning electron microscopy (SEM) or Transmission electron microscopy (TEM).
- ❖ The behavior of the films annealed at  $200^\circ\text{C}$  (473 K) appeared anomalous and should be probed further using other characterization techniques.
- ❖ Annealing in an inert gas.
- ❖ An investigation into the composition of the compounds by carrying out Energy dispersive analysis of X-ray (EDAX) or Neutron activation analysis (NAA).
- ❖ Transport measurements.

## REFERENCES

Ajaya Kumah Singh, Swati Mehra, Gautam Sheel Thoal, (2013). Synthesis of Copper sulphide thin film by Chemical Bath Deposition method and its Characterization. *European chemical Bulletin*,2(8), 518-523

Ali M.S, Khan K.A., and Khan M.S.R., (1995). Quoted by Okereke, N. A., & Ekpunobi, A. J. (2010). STRUCTURAL AND OPTICAL STUDIES OF CHEMICAL BATH DEPOSITED LEAD SELENIDE (PBSE) THIN FILMS. *Journal of Basic Physical Research. Vol, 1(1)*, 13-16.

Al-Mamun, A.B.M.O. and Islam, A.H. Bhuiyan, (2005). Structural, electrical and optical properties of copper selenide thin films deposited by chemical bath technique. *Journal of Materials science in electronics*, volume 16, Issue 5, pp 263-268.

Ashcroft, N. W. (1976). Mermin. ND, 1976. *Solid state physics*, 462-465. Harcourt, Inc: New York.

Asim, N., Ahmadi, S., Alghoul, M. A., Hammadi, F. Y., Saeedfar, K., and Sopian, K. (2014). Research and development aspects on chemical preparation techniques of photo-anodes for dye Sensitized solar cells. *International Journal of Photoenergy*, 2014.

Asogwa, P. U., Ezugwu, S. C., Ezema, F. I., Ekwealor, A. B. C., Ezekoye, B. A., & Osuji, R. U. (2009). Effect of thermal annealing on the band gap and optical properties of chemical bath deposited PbS-CuS thin films. *Journal of optoelectronics and advanced materials*, 11(7), 940-944.

Bagul S.V., Chavahan S.D., Sharma R., (2007). Quoted by Kamoun Alloude Nourhene, Nasr Tarak Ben, Guasch Cathy, Turki Najouna Kamuon, (2010). Optimization of the synthesis and characterizations of chemical bath deposited Cu<sub>2</sub>S thin films. *C.R.Chimie* 13,1364-1369.

Bari, R. H., Ganesan, V., Potadar, S., and Patil, L. A. (2009). Structural, optical and electrical properties of chemically deposited copper selenide films. *Bulletin of Materials Science*, 32(1), 37-42.

Bedir M, Oztas M, Bakkaloglu O F and Ormanci R, (2005). Quoted by Kassim, A., Tee, T. W., Min, H. S., Monohorn, S., & Nagalingam, S. (2010). Effect of bath temperature on the chemical bath deposition of PbSe thin films. *Kathmandu University Journal of Science, Engineering and Technology*, 6(2), 126-132.

Bhuse, V. M., Hankare, P. P., Garadkar, K. M., & Khomane, A. S. (2003). A simple, convenient, low temperature route to grow polycrystalline copper selenide thin films. *Materials chemistry and physics*, 80(1), 82-88.

Bini S., Bindu K., Lakshmi M., Kartha Sudha C., Vijayakuma K.P., Kashiwaba Y., T. Abe, (2000). Quoted by Kamoun Alloude Nourhene, Nasr Tarak Ben, Guasch Cathy, Turki Najouna Kamuon, (2010). Optimization of the synthesis and characterizations of chemical bath deposited Cu<sub>2</sub>S thin films, *C.R.Chimie* 13,1364-1369.

Bioki H. Amrollahi and Zarandi M Borhani, (2011). Quoted by Usuh, Chizomam and Okujagu, Charity, (2014). Influence of Annealing on the Morphology and Optical Properties of Chemically Fabricated Amorphous CuSe Thin Films. *The*

*International Journal Of Engineering And Science (IJES)*, Vol. 3, Issue 6, Pages 43-50.

Chen S.G., Huang Y.F., Liu Y.Q., Xia Q, Liao H.W., Long C.G., (2008). Quoted by Alloude Kamoun Nourhene, Nasr Tarak Ben, Guasch Cathy, Turki Najouna Kamuon, (2010). Optimization of the synthesis and characterizations of chemical bath deposited Cu<sub>2</sub>S thin films. *C.R.Chimie* 13,1364-1369.

Chopra K.L. and Das S.R., (1983). Quoted by Garcia, V. M., Guerrero, L., Nair, M. T. S., & Nair, P. K. (1999). Effect of thermal processing on optical and electrical properties of copper selenide thin films. *Superficies y vacío*, (009), 213-218.

Chopra K.L., and Das S.R., (1983). Thin Film Solar Cells, *Plenium Press*, New York. Transparent conductors – a status review, *Thin Solid Films*, 102, 1 -146.

Chopra, K. L., Kainthla, R.C., Pandra, D.K. and. Thakoor, A. P., (1982). Chemical solution deposition of inorganic films, in *Physics of Thin Films*, G. Hass, Editor. Academic Press: New York.p167-235.

Chu T.L, Chu S.S, Lin S C S C and Yue J, (1984). Quoted by Bari, R. H., Ganesan, V., Potadar, S., & Patil, L. A. (2009). Structural, optical and electrical properties of chemically deposited copper selenide films. *Bulletin of Materials Science*, 32(1), 37-42.

Cody, G. D., (1984). *Semiconductors and Semimetals B*, 21, p. 11.

Cruz J. Santos, Hernández Mayén S. A., Hernández Coronel J. J., Rodríguez Mejía R., Pérez Castanedo R., Delgado Torres G., Sandovala Jiménez S., (2012). Characterization of Cu<sub>x</sub>S Thin Films obtained by CBD technique at different annealing temperatures, *Chalcogenide Letters*, Vol. 9, No. 2, p. 85 – 91.

Dann, S., (2002). Reaction and Characterization of Solids. 1st Edition. p. 55-57.  
New York: John Wiley & Sons, Inc.

Davis, E. A., (1993). Studies of Amorphous Semiconductors Under Pressure. *Japan. J. Appl Phys.* 32, Supp. 32-1, 178-184.

Dimroth, F. (2006). High-efficiency solar cells from III-V compound semiconductors. *Physica Status solidi (c)*, 3(3), 373-379.

Estrada C. A., Nair P. K., Nair M. T. S., Zingaro Ralph A. and Meyers E. A., (1994). Quoted by Lakshmi, M., & Sudha Kartha, C. (2001). *Studies on chemical bath deposited semiconducting copper selenide and iron sulfide thin films useful for photovoltaic applications* (Doctoral dissertation, Department of Physics).

Evans, H.T, (1981). Quoted by Singh, A., Mehra, S., & Thool, G. S. (2013). Synthesis of copper sulphide (CuS) thin film by chemical bath deposition method and its characterization. *European Chemical Bulletin*, 2(8), 518-523.

Fatas , E., T. Garcia, C. Maontemayor, A. Medina , E. Garcia Camarero and F. Arjona , (1985). Formation of Cu<sub>x</sub>S thin films through a chemical bath deposition process. *Material Chemistry and Physics*, 12: p. 121-128.

Filinta Kirmizigül, Emini Güneri and Cebraül Gümüş, (2013). Effects of different deposition conditions on the properties of Cu<sub>2</sub>S thin films, *Philosophical Magazine*, Volume 93, Issue 5.

Fons .P., Niki .S., Yamada .Y. and Oyanagi .H., (1998). Quoted by Bari, R. H., Ganesan, V., Potadar, S., & Patil, L. A. (2009). Structural, optical and electrical properties of chemically deposited copper selenide films. *Bulletin of Materials Science*, 32(1), 37-42.

Froment, M., Cachet, H., Essaoudu, H., Maurin, G. and Cortes, R. (1997). Metal chalcogenide semiconductors growth from aqueous solutions. *Pure and Applied Chemistry*.**69**:p.77-82

Gadave, K. M and C. D. Lokhande, (1993). Formation of  $Cu_xS$  films through a chemical bath deposition process. *Thin Solid Films*, 229: p. 1-4.

Garcia V. M., Nair P. K. and Nair M. T. S., (1999). Quoted by Lakshmi, M., & Sudha Kartha, C. (2001). *Studies on chemical bath deposited semiconducting copper selenide and iron sulfide thin films useful for photovoltaic applications* (Doctoral dissertation, Department of Physics).

Garcia V.M., Nair P.K., Nair M.T.S., (1999). Quoted by Durdu B.G., Alver U., Kucukonder.A, Söşüt.O and Kavgac.M, 2013. Investigation on Zinc Selenide and Copper Selenide Thin Films Produced by Chemical Bath Deposition, *Acta Physica Polonica A*, Vol.12.

Gautier C, Breton G, Nouaoura M, Cambon M, Charar S and Averous M, (1998). Quoted by Kassim, A., Tee, T. W., Min, H. S., Monohorn, S., & Nagalingam, S. (2010). Effect of bath temperature on the chemical bath deposition of PbSe thin films. *Kathmandu University Journal of Science, Engineering and Technology*, 6(2), 126-132.

Goble, R. J, (1985). Quoted by Singh, A., Mehra, S., & Thool, G. S. (2013). Synthesis of copper sulphide ( $CuS$ ) thin film by chemical bath deposition method and its characterization. *European Chemical Bulletin*, 2(8), 518-523.

Gorer, S and G. Hodes. (1994). Quantum size effects in the study of chemical solution deposition mechanisms of semiconductor films. *Journal of Physical Chemistry*. **98**:p.5338-5346.

Gosavi, S. R., Deshpande, N. G., Gudage, Y. G., & Sharma, R. (2008). Physical, optical and electrical properties of copper selenide (CuSe) thin films deposited by solution growth technique at room temperature. *Journal of Alloys and Compounds*, 448(1), 344-348.

Grozdanov, (1994). Quoted by Lakshmi, M., & Sudha Kartha, C. (2001). *Studies on chemical bath deposited semiconducting copper selenide and iron sulfide thin films useful for photovoltaic applications* (Doctoral dissertation, Department of Physics).

Grundmann, M. (2006). The physics of semiconductors. by WT Thodes, HE Stanley, R. Needs:(Springer, Berlin, 2010) p, 29-62

Gurin, V. S., Alexeenko, A. A., Tyavlovskaya, E. A., & Kasparov, K. N. (2008). Sol-gel silica thin films with copper selenide. *Thin Solid Films*, 516(7), 1464-1467.

Haram S K, Santhanam K S V, Neumann-Spallart M and Levy-Clement C, (1992). Quoted by Durdu B.G., Alver U., Kucukonder.A, Söşüt.O and Kavgac.M, 2013. Investigation on Zinc Selenide and Copper Selenide Thin Films Produced by Chemical Bath Deposition, *Acta Physica Polonica A*, Vol.12.

Haram S. K, Santhanam K. S. V, Neumann-Spallart .M. and Levy-Clement C., (1992). Quoted by Bari, R. H., Ganesan, V., Potadar, S., & Patil, L. A. (2009). Structural, optical and electrical properties of chemically deposited copper selenide films. *Bulletin of Materials Science*, 32(1), 37-42.

Haram S.K. and Santhanam KSV, (1994). Quoted by Garcia, V. M., Guerrero, L., Nair, M. T. S., & Nair, P. K. (1999). Effect of thermal processing on optical and electrical properties of copper selenide thin films. *Superficies y vacío*, (009), 213-218.

Hermann A.M. and Fabick L., (1983). Quoted by Garcia, V. M., Guerrero, L., Nair, M. T. S., & Nair, P. K. (1999). Effect of thermal processing on optical and electrical properties of copper selenide thin films. *Superficies y vacío*, (009), 213-218.

Heyding, R. D. (1966). The copper/selenium system. *Canadian Journal of Chemistry*, 44(10), 1233-1236.

Hodes, G., (2002), *Chemical Solution Deposition of Semiconductor Films*: Marcel Dekker, Inc. 270 Madison Avenue, New York, NY 10016.

[http://ej.iop.org/images/0953-8984/24/1/015701/Full/cm398459f1\\_online.jpg](http://ej.iop.org/images/0953-8984/24/1/015701/Full/cm398459f1_online.jpg)  
(Accessed: 24<sup>th</sup> July, 2014).

<http://prism.mit.edu/xray> (Accessed: 11<sup>th</sup> June, 2014)

[http://shodhganga.inflibnet.ac.in/bitstream/10603/4025/8/08\\_chapter%202.pdf](http://shodhganga.inflibnet.ac.in/bitstream/10603/4025/8/08_chapter%202.pdf)  
(Accessed: 24<sup>th</sup> July, 2014)

<http://www.answers.com/topic/crystal> (Accessed: 30<sup>th</sup> July, 2014)

[http://en.m.wikipedia.org/wiki/file:Kristallstruktur\\_Chalkosin.png](http://en.m.wikipedia.org/wiki/file:Kristallstruktur_Chalkosin.png) (Accessed: 8<sup>th</sup> February, 2014)

[http://en.wikipedia.org/wiki/characterization\\_material\\_science](http://en.wikipedia.org/wiki/characterization_material_science) (Accessed: 28<sup>th</sup> July, 2014)

[http://en.wikipedia.org/wiki/Sputter\\_deposition](http://en.wikipedia.org/wiki/Sputter_deposition) (Accessed: 24<sup>th</sup> July, 2014)

<https://www.mtm.kuleuven.be/Onderzoek/Ceramics/EPD> Electrophoretic Deposition (EPD) – Departement Metaalkunde en Toegepaste Materiaalkunde KU Leuven (Accessed: 24<sup>th</sup> July, 2014)

[http://www.nature.com/nmat/journal/v11/n5/fig\\_tab/nmat3273\\_F1.html](http://www.nature.com/nmat/journal/v11/n5/fig_tab/nmat3273_F1.html). Crystal structure of Cu<sub>2</sub>Se at high temperatures ( $\beta$ -phase) with a cubic anti-fluorite structure: Copper ion liquid-like thermoelectrics. *Nature Materials*. Nature Publishing Group. (Accessed on: 24<sup>th</sup> July, 2014)

<http://www.precisionfab.net/tutorials02.aspx>. Tutorials | Precision Fabricators. Schematic of a typical low pressure hot wall CVD reactor used in coating silicon substrates. Adapted from H. O. Pierson, *Handbook of Chemical Vapor Deposition*, Noyes Publications, Park Ridge (1992). (Accessed: 30<sup>th</sup> July, 2014).

Ilenikhena P.A., (2008), Comparative studies of Improved Chemical Bath deposited Copper sulphide and Zinc Sulphide thin films at 320K and Possible Application, *African Physical Review* 2:0007

Isac. I, Duta. A, Kriza. A, Manolade. S, Nanu. M, (2007). Quoted by Kamoun Alloude Nourhene, Nasr Tarak Ben, Guasch Cathy, Turki Najouna Kamuon, (2010). Optimization of the synthesis and characterizations of chemical bath deposited Cu<sub>2</sub>S thin films, *C.R.Chimie* 13,1364-1369.

Jagminas, A., Juškėnas, R., Gailiūtė, I., Statkutė, G., & Tomašiūnas, R. (2006). Electrochemical synthesis and optical characterization of copper selenide nanowire arrays within the alumina pores. *Journal of crystal growth*, 294(2), 343-348.

Juška, G., Gulbinas, V., & Jagminas, A. (2010). Transient absorption of copper selenide nanowires of different stoichiometry. *Lithuanian Journal of Physics*, 50(2).

Kale, S.S. and Lokhande, C.D., (2000). Quoted by Moradian, R., Ghobadi, N., Roushani, M., & Shamsipur, M. (2011). Synthesis, characterization and size dependent energy band gap of binary CdSe quantum dot and its nanoparticle film. *Journal of the Iranian Chemical Society*, 8(1), S104-S109.

Kashida S and Akai J, (1988). Quoted by Bari, R. H., Ganesan, V., Potadar, S., & Patil, L. A. (2009). Structural, optical and electrical properties of chemically deposited copper selenide films. *Bulletin of Materials Science*, 32(1), 37-42.

Kassim, A., Nagalingam, S., Tee T.W., Sharif, A.M., Abdulah, D. K., Elos M. J and Min, H.S., (2009). Effect of Deposition Period and pH on Chemical Deposition  $Cu_nS_4$  thin Films. *Philippians Journal of science* 138 (2), 161-168.

Khomane A. S., (2012). Synthesis and characterization of chemically deposited  $Cu_{2-x}Se$  thin films. *Archives of Applied Science Research*, 4 (4):1857-1863

Kumar, V., Sharma, M. K., Gaur, J., & Sharma, T. P. (2008). Polycrystalline ZnS thin films by screen printing method and its characterization. *Chalcogenide lett*, 5(11), 289-295.

Lakshmi M., Bindu K., Bini S., Vijayakumar K.P., Kartha C.S., Abe T., Kashiwaba Y., (2001). Quoted by Durdu B.G., Alver .U, Kucukonder .A, Söşüt .O. and Kavgac .M., (2013). Investigation on Zinc Selenide and Copper Selenide Thin Films Produced by Chemical Bath Deposition. *Acta Physica Polonica A*, Vol.124.

Lakshmikummar S T, (1994). Quoted by Bari, R. H., Ganesan, V., Potadar, S., & Patil, L. A. (2009). Structural, optical and electrical properties of chemically deposited copper selenide films. *Bulletin of Materials Science*, 32(1), 37-42.

Levy-Clement C, Neumann-Spallart M, Haram S K and Santhanam K S V, (1997). Quoted by Bari, R. H., Ganesan, V., Potadar, S., & Patil, L. A. (2009). Structural, optical and electrical properties of chemically deposited copper selenide films. *Bulletin of Materials Science*, 32(1), 37-42.

Lincot , D. Froment, M and Cachet, H., (1999). Chemical deposition of chalcogenide thin films from solution. *Advances in Electrochemical Science and engineering*, 6, pp 165-235.

Massaccesi S., Sanchez S. and Vedd J., (1993). Quoted Garcia, V. M., Guerrero, L., Nair, M. T. S., & Nair, P. K. (1999). Effect of thermal processing on optical and electrical properties of copper selenide thin films. *Superficies y vacío*, (009), 213-218.

Mott, N. F. and Davis, E. A., (1979). Electronic processes in non-crystalline materials, 2nd Ed., Clarendon Press, Oxford.

Munce C.G., Parker G.K. , Holt S.A., Hope G.A., (2007). Quoted by Kamoun Alloude Nourhene, Nasr Tarak Ben, Guasch Cathy, Turki Najouna Kamuon, (2010). Optimization of the synthesis and characterizations of chemical bath deposited Cu<sub>2</sub>S thin films. *C.R.Chimie* 13,1364-1369.

Murali, K. R., & Xavier, R. J. (2009). Characteristics of brush electroplated copper selenide thin films. *Chalcogenide Letters*, 6(12), 683-687.

Musembi, R., Aduda, B., Mwabora, J., Rusu, M., Fostiropoulos, K., and Lux-Steiner, M. (2013). Effect of Recombination on Series Resistance in eta Solar Cell Modified with In (OH) xSy Buffer Layer. *International Journal of Energy Engineering*, 3(3), 183-189.

Nadeem, M.Y, Ahmed, W., Wasiq, M.F., (2005). ZnS Thin Films – An Overview. *J of Research (science); Buhauddin Zakaniya University, Multan, Pakistan*-Vol.16, pp105.

Neamen, D. A. Semiconductor Physics and Devices: Basic Principles, 2003. *McGraw-Hill New York*, 449-509.

O'Brien R N and Santhanam K S V, (1992). Quoted by Bari, R. H., Ganesan, V., Potadar, S., & Patil, L. A. (2009). Structural, optical and electrical properties of chemically deposited copper selenide films. *Bulletin of Materials Science*, 32(1), 37-42.

Offiah, S. U., Ugwoke, P. E., Ekwealor, A. B. C., Ezugwu, S. C., Osuji, R. U., & Ezema, F. I. (2012). Structural and spectral analysis of chemical bath deposited copper sulfide thin films for solar energy conversions. *Digest Journal Of Nano Materials And Bio Structures*, 7(1), 165-173.

Okereke, N. A., & Ekpunobi, A. J. (2011). XRD and UV-VIS-IR Studies of Chemically-Synthesized Copper Selenide Thin Films. *Research Journal of Chemical Sciences* ISSN, 2231, 606X.

Okimura H., Matsumae T. and Makabe R., (1980). Quoted by Lakshmi, M., & Sudha Kartha, C. (2001). *Studies on chemical bath deposited semiconducting copper selenide and iron sulfide thin films useful for photovoltaic applications* (Doctoral dissertation, Department of Physics).

Omran, A. H., & Jaafer, M. D. (2013). Annealing Effect on The Structural and Optical Properties of CuS Thin Film Prepared By Chemical Bath Deposition (CBD). *Journal of Kufa-Physics*, 5(1).

Parkin I.P., (1996) Quoted by Kamoun Alloude Nourhene, Nasr Tarak Ben, Guasch Cathy, Turki Najouna Kamuon, (2010). Optimization of the synthesis and characterizations of chemical bath deposited Cu<sub>2</sub>S thin films, *C.R.Chimie* 13,1364-1369.

Parkin I.P., (1996). Quoted by Khomane A. S., (2012). Synthesis and characterization of chemically deposited Cu<sub>2-x</sub>Se thin films, *Archives of Applied Science Research*, 4 (4):1857-1863

Pathan H.M., Desai J.D., Lokhande C.D., (2002). Quoted by Kamoun Alloude Nourhene, Nasr Tarak Ben, Guasch Cathy, Turki Najouna Kamuon, (2010). Optimization of the synthesis and characterizations of chemical bath deposited Cu<sub>2</sub>S thin films. *C.R.Chimie* 13,1364-1369.

Pathan, H. M., & Lokhande, C. D. (2004). Deposition of metal chalcogenide thin films by successive ionic layer adsorption and reaction (SILAR) method. *Bulletin of Materials Science*, 27(2), 85-111.

Pathan, H. M., Lokhande, C. D., Amalnerkar, D. P., & Seth, T. (2003). Modified chemical deposition and physico-chemical properties of copper (I) selenide thin films. *Applied surface science*, 211(1), 48-56.

Pawan K., Aravind K., Dixit P. N., Sharma T. P., (2006). Quoted by Offiah, S. U., Ugwoke, P. E., Ekwealor, A. B. C., Ezugwu, S. C., Osuji, R. U., & Ezema, F. I. (2012). Structural and spectral analysis of chemical bath deposited copper sulfide thin films for solar energy conversions. *Digest Journal Of Nano Materials And Bio Structures*, 7(1), 165-173.

Pop, A. E., Batin, M. N., & Popescu, V. (2011). THE INFLUENCE OF ANNEALING TEMPERATURE ON COPPER SULPHIDE  $Cu_{(x)}S$  OBTAINED BY CHEMICAL PRECIPITATION. *Powder Metallurgy Progress*, 11(3-4), 197-200.

Rajesh Desapogu, R Rajesh Chandrakanth and C S Sunandana, (2013). Annealing Effects on the Properties of Copper Selenide Thin Films for Thermoelectric Applications, *IOSR Journal of Applied Physics (IOSR-JAP) e-ISSN: 2278-4861. Volume 4, Issue 5, PP 65-71, www.iosrjournals.org.*

Razak, A. and Sharin, M. F. (2007). *Electrophoretic deposition and characterization of copper selenide thin films* (Doctoral dissertation, Universiti Putra Malaysia).

Redmond, W.A. X-Ray Diffraction." *Microsoft® Student 2009*. Microsoft Corporation, 2008.

Richard C. N., (1978). Quoted by Offiah, S. U., Ugwoke, P. E., Ekwealor, A. B. C., Ezugwu, S. C., Osuji, R. U., & Ezema, F. I. (2012). Structural and spectral analysis of chemical bath deposited copper sulfide thin films for solar energy conversions. *Digest Journal Of Nano Materials And Bio Structures*, 7(1), 165-173.

Rothwarf, A., & Barnett, A. M. (1977). Design analysis of the thin-film  $CdS-Cu_2S$  solar cell. *Electron Devices, IEEE Transactions on*, 24(4), 381-387.

Sankapal, B. R., Sartale, S. D., Lokhande, C. D., & Ennaoui, A. (2004). Chemical synthesis of Cd-free wide band gap materials for solar cells. *Solar energy materials and solar cells*, 83(4), 447-458.

Scheider S., Ireland J.R., Hersam M.C, Mark T.J., (2007). Quoted by Kamoun Alloude Nourhene, Nasr Tarak Ben, Guasch Cathy, Turki Najouna Kamuon, (2010).

Optimization of the synthesis and characterizations of chemical bath deposited  $\text{Cu}_2\text{S}$  thin films. *C.R.Chimie* 13,1364-1369.

Scherrer P. Bestimmung der Grösse und der inneren Struktur von Kolloidteilchen mittels Röntgenstrahlen [Determination of the size and internal structure of colloidal particles using X-rays]. *Nachr Ges Wiss Goettingen, Math-Phys Kl.* 1918;1918:98-100. German.

Schroder, D. K. (1998). *Semiconductor material and device characterization*. John Wiley & Sons, New York.

Singh, J. (Ed.). (2006). *Optical properties of condensed matter and applications* (Vol. 6). John Wiley & Sons: England.

Singh, J. and Shimakawa, K. (Eds.) (2003). *Advances in amorphous semiconductors*. CRC Press. (Taylor and Francis, London), p.294

Sorokin G. P., Papshev Hu. M. and Oush P. T., Sov., (1996). Quoted by Lakshmi, M., & Sudha Kartha, C. (2001). *Studies on chemical bath deposited semiconducting copper selenide and iron sulfide thin films useful for photovoltaic applications* (Doctoral dissertation, Department of Physics).

Stern, F., (1963). Quoted by Anuar, K. Tan, W.T. Jelas, M. Ho, S.M. and Gwee, S.Y., (2010). Effects of deposition period on the Properties of  $\text{FeS}_2$  Thin films by Chemical Bath Deposition Method, *Thammasat Int. J. Sc. Tech.*, 15, 2, p 64

Tauc, J., (1974). (Ed.), *Amorphous and Liquid Semiconductors*, Plenum: New York, p. 159.

Tell B., Weigand J.J., (1977). Quoted Khomane A. S., (2012). Synthesis and characterization of chemically deposited  $\text{Cu}_{2-x}\text{Se}$  thin films, *Archives of Applied Science Research*, 4 (4):1857-1863

Thewlis J., (1979). Quoted by Nadeem, M. Y., Waqas, A., & Wasiq, M. F. (2005). ZnS thin films—an overview. *Journal of research science*, 16, 105-112.

Toneje A and Toneje A M, (1981). Quoted by Bari, R. H., Ganesan, V., Potadar, S., & Patil, L. A. (2009). Structural, optical and electrical properties of chemically deposited copper selenide films. *Bulletin of Materials Science*, 32(1), 37-42.

Ubale, A. U., Sangawar, V. S., & Kulkarni, D. K. (2007). Size dependent optical characteristics of chemically deposited nanostructured ZnS thin films. *Bulletin of Materials Science*, 30(2), 147-151.

Uhuegbu, C. C. , (2010). Quoted by Offiah, S. U., Ugwoke, P. E., Ekwealor, A. B. C., Ezugwu, S. C., Osuji, R. U., & Ezema, F. I. (2012). Structural and spectral analysis of chemical bath deposited copper sulfide thin films for solar energy conversions. *Digest Journal Of Nano Materials And Bio Structures*, 7(1), 165-173.

Usoh, Chizomam and Okujagu, Charity, (2014). Influence of Annealing on the Morphology and Optical Properties of Chemically Fabricated Amorphous CuSe Thin Films , *The International Journal Of Engineering And Science (IJES)*, Volume 3, Issue 6, Pages 43-50.

Varkey A.J., (1989). Chemical bath deposition of  $\text{Cu}_x\text{S}$  thin films using ethylenediaminetetraacetic acid (EDTA) as complexing agent, *Solar Energy Material*, 19: p. 415-420.

Vučić, Z., Horvatić, V., & Milat, O. (1984). Dilatometric study of nonstoichiometric copper selenide  $\text{Cu}_{2-x}\text{Se}$ . *Solid State Ionics*, 13(2), 127-133.

Wang Y.J., Tsai A.T., Yang C.S., (2009). Quoted by Kamoun Alloude Nourhene, Nasr Tarak Ben, Guasch Cathy, Turki Najouna Kamuon, (2010). Optimization of the synthesis and characterizations of chemical bath deposited  $\text{Cu}_2\text{S}$  thin films, *C.R.Chimie* 13,1364-1369.

Wood, D. L., & Tauc, J. S. (1972). Weak absorption tails in amorphous semiconductors. *Physical Review B*, 5(8), 3144.

Wu, Y., Wadia, C., Ma, W., Sadler, B., & Alivisatos, A. P. (2008). Synthesis and photovoltaic application of copper (I) sulfide nanocrystals. *Nano letters*, 8(8), 2551-2555.

www.AZoM.com (Accessed: 22<sup>nd</sup> May, 2014).

Wyckoff, R. W. G., (1965). Quoted by Ajaya Kumar Sing, Swati Mehra, Gautam Sheel Thoo, (2013). Synthesis of Copper sulphide ( $\text{CuS}$ ) thin film by chemical bath deposition method and its characterization, *European Chemical Bulletin*, 2(8),518-523

Yacobi, B. G. (2003). Applications of Semiconductors. *Semiconductor Materials: An Introduction to Basic Principles*, 107-134. Kluwer/ Plenum: New York

Yacobi, B. G., (2004). *Semiconductor Materials: An Introduction to Basic Principles*, pp.1-3, 154-157, 107. Kluwer: New York

Young, H. D. and Freedman, R. A. (2008). *University Physics*, Vol. I. Pearson, Addison Wesley.

Zainal, Z., Nagalingam, S., & Loo, T. C. (2005). Copper selenide thin films prepared using combination of chemical precipitation and dip coating method. *Materials Letters*, 59(11), 1391-1394.

Zinoviev, K. V., & Zelaya-Angel, O. (2001). Influence of low temperature thermal annealing on the dark resistivity of chemical bath deposited CdS films. *Materials chemistry and physics*, 70(1), 100-102.

KNUST

